Development of Laboratory and Field Scale

Passive Vibration Assisted Rotary Drilling Tools

By

Brock Gillis

A Thesis submitted to the

School of Graduate Studies

In partial fulfillment of the requirements for the degree of

Master of Engineering

Faculty of Engineering and Applied Science

Memorial University of Newfoundland

October 2019

Abstract

The Drilling Technology Laboratory (DTL) at Memorial University of Newfoundland has been focused on increasing drilling efficiency through the utilization of downhole vibrations, also known as Vibration Assisted Rotary Drilling (VARD). The pursuit of VARD technologies is split between active and passive vibrations and the current thesis looks at the design, development, and testing of a Passive Vibration Assisted Rotary Drilling tool (pVARD). The pVARD tool acts as a spring and damper inside the bottom hole assembly of the drill string. It is a system that is tuned to utilize the natural vibrations of the drilling process to increase drilling efficiency and rate of penetration.

Two different tools were designed. First, a laboratory scale tool designed to allow analysis into pVARD to be performed on the DTL's inhouse small drilling simulator. This would allow for rapid testing of many spring damper configurations. The second, a field scale tool, that would be used with six-inch drill bits in the DTL's first field trial of VARD technology. Powered by a water well drilling rig, this tool would be used to drill shale and granite and explore the pVARD technology on an industrial scale. Both tools required the design of axial and torque taking members as well as the arrangement of the spring damper system. Specific design attention was paid to making the tools easily reconfigurable so that different spring damper arrangements could be tested, both in the lab, and the field.

This investigation explores the testing results of these two tools as compared to one another, as well as learning from the operation of them in the field and how these learning will be used to improve the next generation of pVARD tools.

Keywords: oil and gas, drilling, drill string, vibration, efficiency, drilling tools

Table of Contents

List of Figures

List of Tables

1 Introduction

1.1 **VARD and the Petrochemical Industry**

The petrochemical industry is responsible for approximately 7.5% of Canadian GDP (NRC Energy Markets Factbook). The petrochemical industry is composed of five main segments; exploration, extraction, refining, transportation, and marketing. The Drilling Technology Laboratory (DTL) works specifically within the first two segments, exploration and extraction, where drilling is the main technique used to access petrochemical reserves. Drilling constitutes a large cost to operators looking to access reserves and with approximately two thousand drilling operations on the go around the world (Baker Hughes, 2019), there is great value in making the process more efficient.

It is the goal of the operator and service companies to make every aspect of the drilling process as efficient as possible. Every possible variable is tuned to optimize ROP (rate of penetration). Weight on bit and rotary speed are balanced against bit wear to optimize the ROP without the need to replace the bit, which is costly in both dollars and time. This same type of balancing-act is conducted with the many variables that affect the speed at which a well is drilled. The drilling industry currently uses drill-off and pump-off tests to optimize weight on bit, rotary speed and bit hydraulics during drilling operations for maximum efficiency.

The Vibration Assisted Rotary Drilling (VARD) project at the Drilling Technology Laboratory aims to further improve drilling efficiency by understanding one key variable, drill string vibration. How drill string vibrations can affect rock penetration, hole cleaning and bit wear. This knowledge will help in the development of a suite of

drilling tools for increasing drilling efficiency beyond the current limit of optimizing the existing drilling parameters.

1.2 Current Project

This thesis covers the investigation of passive vibration assisted rotary drilling or "pVARD". The main concept behind pVARD is that drilling efficiency can be improved by the inclusion of a passive tool in the bottom hole assembly (BHA). This passive tool could enhance or dampen the natural vibrations generated by the drilling operation. The DTL's pVARD tool is modeled after typical downhole shock absorbers that are included in some bottom hole assemblies. These "shock tools" improve the reliability of the BHA by reducing vibrations transmitted to the drill string and drilling tools. The DTL has fabricated two pVARD tools at Memorial University, one laboratory scale tool to be used with a small bit and a second field scale tool to be used with an industrial sized drill bit.

Testing these tools under different drilling situations allows measurement of ROP, but ROP alone is not a measure of drilling efficiency. This project utilizes a specific energy measurement that considers the different parameters that lead to the measured ROP to examine the effect of the pVARD tool as compared to standard drilling performance. The testing follows a similar method to the standard drill off tests where the weight on bit is incrementally changed and the time to drill a set distance is recorded. This allows for the calculation of ROP, and with ROP, and the other drilling parameters, the calculation of specific energy.

This work builds on the previous work of the DTL and its members. Early DTL experiments used coring bits at atmospheric conditions to drill rock samples. A vibrating

plate was used to vibrate the sample as it was being drilled to look for ROP improvements. Next these experiments progressed to drilling these samples under pressure in simulated down hole conditions. Before the current experiments, testing was carried out to look at the effect of adjustable compliance. The sample was mounted on a fixture that allowed it to move with the cutting action of the bit. These initial tests into passive vibration led to the current project that aims to evaluate the pVARD technology in the drill string at laboratory and industrial scale.

1.3 Thesis Outline

This thesis looks at the design, development and testing of the Passive Vibration Assisted Rotary Drilling tool (pVARD). It looks at the evaluation of the tool in both the laboratory setting as well as in field trials.

Section 2 will briefly describe the current state of knowledge around this technology, the issues faced, measurements used, and learnings from previous generations of the technology.

Section 3 covers the design and development of both the laboratory scale and field trial scale pVARD tools and how they are constructed.

Section 4 explains the field trail organization and testing. The location where field trials took place as well as the geological makeup of the field trial site.

Section 5 describes the results of both laboratory scale and field trial testing and discusses the evaluation of these results using mechanical specific energy.

Section 6 suggests improvements to the field trial tool for the next design iteration.

Section 7 closes out the thesis with a written conclusion and notes on future research.

2 Literature Review

This section gives a brief overview of the subject matter surrounding this thesis topic.

2.1 **Drilling Efficiency**

Wilmot (Wilmot, et al., 2010) defines drilling efficiency as "the construction and delivery of a useable well, while achieving the operational conditions needed to achieve the lowest cost imprint". Essentially stating that there is no single performance qualifier (PQ) that equates to drilling efficiency and that all PQ's and their effect on each other must be evaluated to give the highest efficiency.

Attempts at quantifying drilling efficiency have previously tied the measure to cost per foot (CPF), feet per day (FPD), and mechanical specific energy (MSE).

$$CPF = \frac{1}{ROP} \times \left[\left(\frac{BC}{t}\right) + RR \times \left(1 + \frac{Tt}{t}\right)\right]$$

$$FPD = ROP_{AVG} \times 24$$

$$MSE = \frac{WOB}{A_B} + \frac{120 \times \pi \times RPM \times T}{A_B \times ROP}$$

Where "ROP" is rate of penetration, "BC" is bit cost, "t" is time, "RR" is the rig rate, "Tt" is Trip Time, "WOB" is weight on bit, "AB" is the bit area, "RPM" is rotations per minute, and "T" is torque.

These metrics while useful do not give a complete picture. One must evaluate all the PQ's together to come up with an effective picture of drilling efficiency. The PQ's as Wilmot laid out are:

- Footage drilled per bottom hole assembly
- Downhole tool life

- Vibrations control
- Durability
- Steering efficiency
- Directional responsiveness
- Rate of penetration (ROP)
- Borehole quality

When examining the PQ's together it is easy to recognize that increasing ROP at the expense of downhole tool life could result in a lower drilling efficiency even though the factors shown above such as MSE improve with increased ROP. For ROP increases to positively affect drilling efficiency the increases must be seen in the average ROP. Increases in instantaneous ROP can lead to deterioration of down hole tool life, unwanted vibrations and unplanned events such as trips to replace tooling leading to a decrease in average ROP as well as a decrease in drilling efficiency.

2.2 Average Rate of Penetration

Rate of penetration is defined as "advancement per unit time, while the drill bit is on bottom and drilling ahead" (Wilmot, et al., 2010). Average ROP is measured over the complete drilled interval.

Pessier (Pessier, Walace, Oueslati, & Baker Hughes, 2012) describes some of the drilling conditions that can affect ROP. Rock lithology impacts ROP through MSE. Higher strength material requires more MSE which leads to lower depth of cut and lower

ROP. Lithology can also impact ROP by causing the bit to cut with less efficient cutting modes, as well as the harder rock may more easily trigger stick slip.

Bit type and condition also affect ROP. Pessier noted that the more conventional short profile bit they tested had a much larger operating window than the long parabolic profile. The short profile allowed drilling with more weight on bit which equated to higher ROP and increased drilling efficiency. Intuitively ROP drops off and MSE rises as a bit wears. Also, dull bits can trigger stick slip vibrations at lower RPM. Conventionally stick slip is fought by increasing RPM and decreasing WOB which causes an exponential decrease in ROP.

By graphing power, the relationship between MSE and ROP can be intuitively investigated throughout drilling operations. This method can illustrate graphically how PQ's affect drilling performance and ROP. Fig. 1 shows a power graph for a US land Rig color coded for drilling depth (Pessier, Walace, Oueslati, & Baker Hughes, 2012).

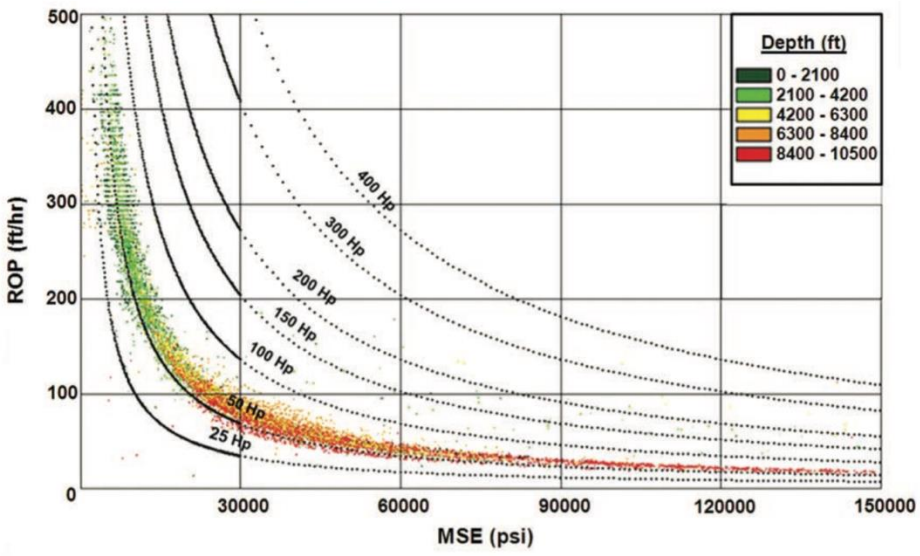

Fig. 1: Power Graph of US land Rig (Pessier, Walace, Oueslati, & Baker Hughes, 2012)

2.3 Vibration and Rock Penetration

2.3.1 Types of Down Hole Vibrations

In 1964 Feenstra (R.Feenstra, 1964) divided down hole vibrations into the four following categories:

1. Axial

   Axial vibrations are motions along the drill string axis. Also known as “bit bounce”, these vibrations are commonly caused by large variations in the weight on bit. Varying weight on bit can result in a rate of penetration reduction, as well as damage to the bit and BHA components.

2. Torsional

   Torsional vibrations, or “stick slip”, is a rotary motion around the axis of the drill string. This occurs when the rock resists the cutting torque to the point the bit slows, and in some cases stops. The drill string twists along its length storing energy and increasing the torque at the bit. When the built-up torque overcomes the rock strength, the drill string unwinds, and the bit rotates. The stored rotational energy is expended and the bit once again slows in contact with the rock and the process is repeated.

3. Lateral

   Lateral vibrations are side to side bending motions of the drill sting. These motions are usually caused by eccentric bit rotation.

4. Eccentered

Eccentered vibration combines the torsional vibration of stick-slip with side to side bending vibration creating eccentered vibration or BHA whirl.

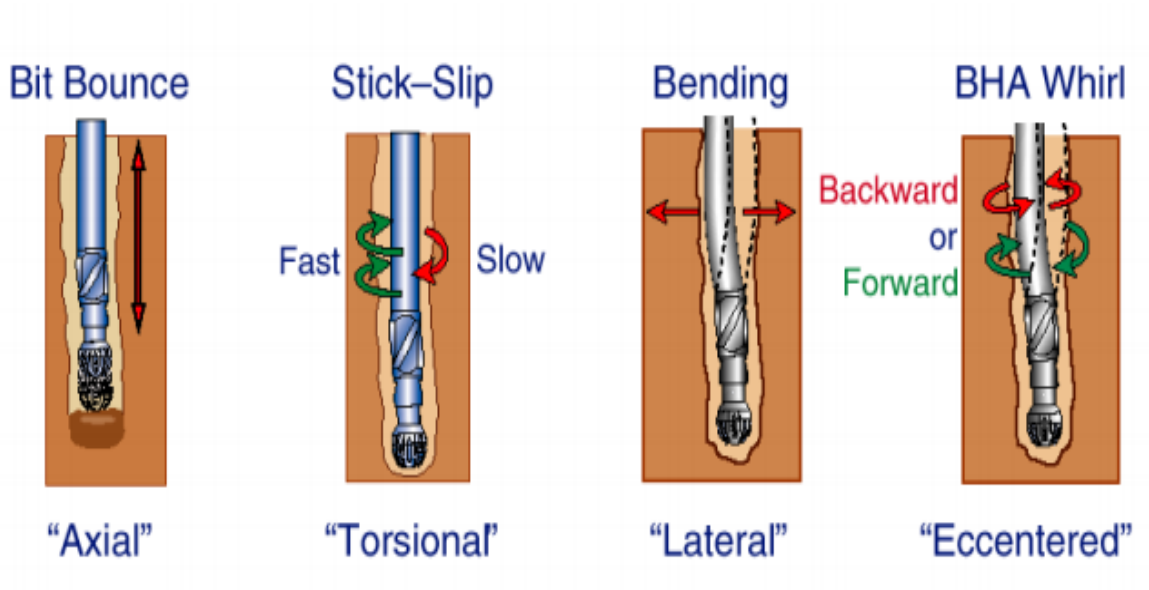

Fig. 2: Vibration Categories (Ashely, McNary, & Tomlinson, 2001)

2.3.2 Vibration's Effect on ROP

Utilizing vibration to increase ROP has been studied for over half a century. Eskin et al (Eskin, 1995) described early study into the effect of vibration on ROP. In 1957 Burkap et al. (Barkap, 1957) showed results using axial vibrations between 67 and 83 Hz while drilling at various rotating speeds in red granite. These experiments demonstrated the possibility of positively affecting ROP through application of axial vibrations. Baidyuk et al. (Baidyuk, 1993) showed that pulsed loading of the weight on bit can have a positive effect on ROP. In their experiment a small cutter bit was rotated at a constant

speed while it underwent cyclic weight on bit loading. The loading frequency was also varied, between 1 and 24 times that of the rotational speed.

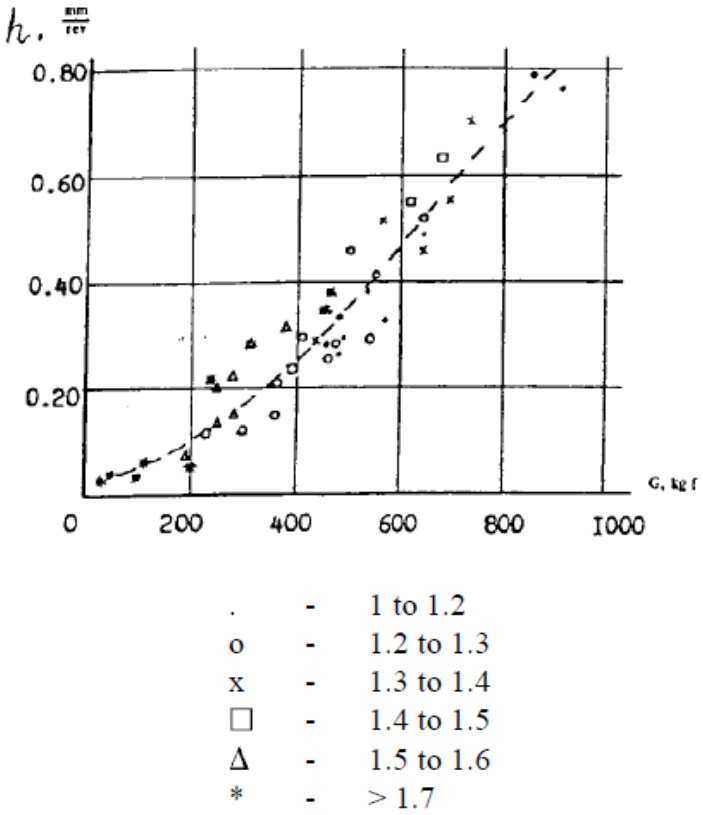

Fig. 3: Experimental Drilling Results (Baidyuk, 1993)

The above graph shows experimental results from Baidyuk et al. Fig. 3 shows penetration per revolution (h) on the y-axis versus the weight on bit on the x-axis. The different points are showing various ratios of vibration force amplitude (ΔG) over WOB(Gc).

More recent studies into the effect of vibration on rate of penetration have shown that there are potential gains to be made in ROP. Li et al. (Heng Li, 2010) investigated the effect of vibration on a coring bit as well as a full-face bit. Li kept vibration frequency constant while varying rotary speed, weight on bit and vibration amplitude. Fig. 4 shows Li's results using the coring bit. Li concluded that the relationship between vibration

amplitude and ROP was non-linear, and that by varying the amplitude ROP could be optimized.

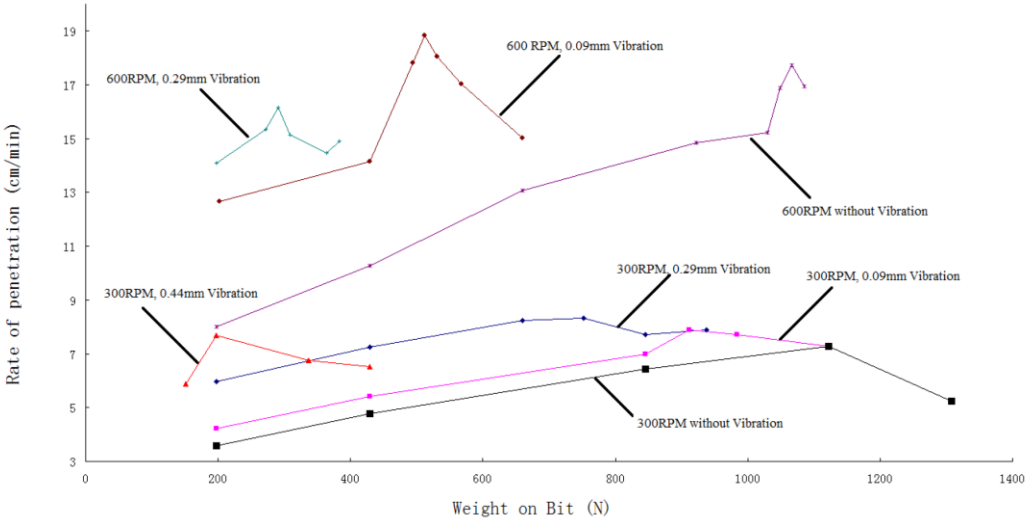

Fig. 4: Experimental results of vibration assisted rotary drilling (Li, 2011)

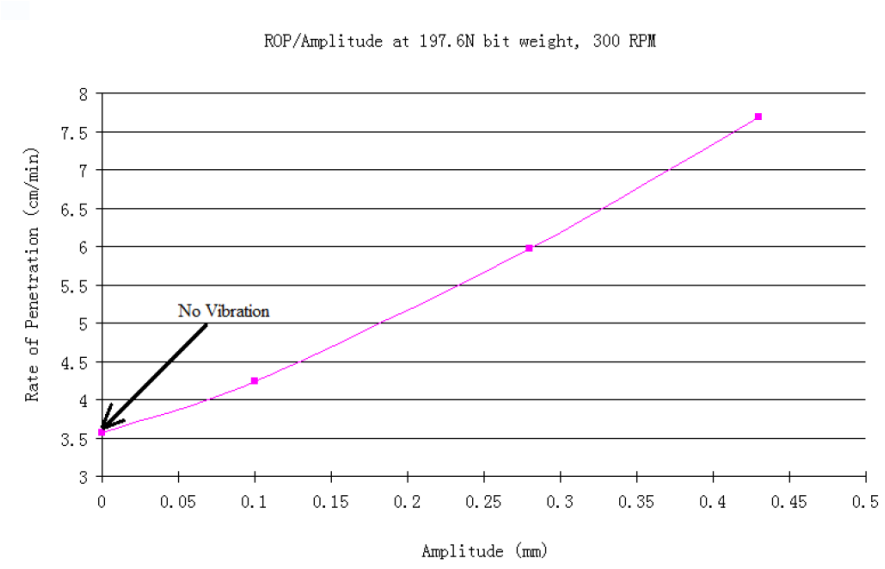

Fig. 5: Effect of vibration amplitude on ROP with constant WOB and RPM (Li, 2011)

Li et al. saw similar results using the full-face bit with the same vibration setup. ROP increases can be seen in Fig. 5. Li et al. concluded that increasing vibration amplitude leads to an increase in ROP until the founder point is reached.

Building on Li's work, Yusuf Babtunde et al (Yusuf Babatunde, 2011) explored varying the vibration frequency as well as the amplitude with diamond drag bits. Fig. 6 shows the ROP increases achieved at a constant vibration amplitude at different frequencies.

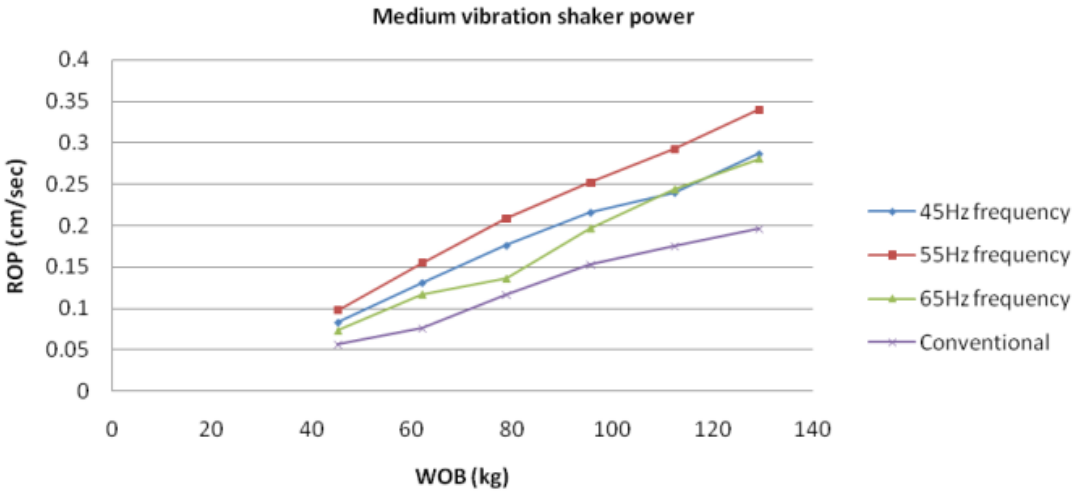

Fig. 6: WOB vs. ROP for a drag bit under vibration (Yusuf Babatunde, 2011)

Babtunde concluded that significant increases in ROP could be made with diamond drag bits though the use of applied vibration and that increased vibration amplitude increased ROP. Babtunde also suggests that in his experiments bit life was not affected significantly enough to reduce overall drilling efficiency.

Further research was done into applied vibration using distinct element modeling or DEM. Khorshidian et al (Khorshidian, 2012)describes simulations using DEM of a single PDC cutter on Carthage Limestone. Their simulations showed that axial vibration

has two possible effects on cutter penetration. Firstly, the vibration can impose impact loading on the rock causing cratering as shown in Fig. 7 and secondly after exceeding some optimal point of vibration amplitude there is an increase in mechanical specific energy. They concluded that the improvement in penetration was due to a reduction in the force required to advance the cutter horizontally and that the impact loading caused the formation of larger chips.

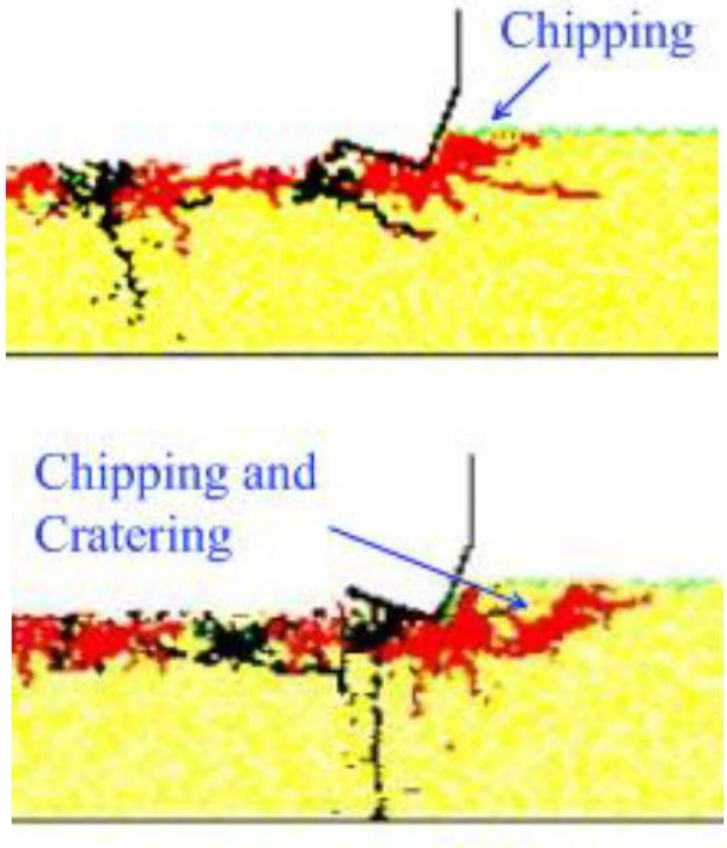

Fig. 7: Images from Khorshidians DEM models (Khorshidian, 2012)

Upper Image: Chipping under low vertical force oscillations Lower Image: Cratering under high vertical force oscillations

Wang et al. (Wang, Butt, & Yang, 2013) also simulated applied vibration. They used CFD simulation to study a Downhole Oscillating Device or DOD and a one-degree of freedom spring, mass, damper model (Fig. 8) to simulate the effect of the DOD on the BHA.

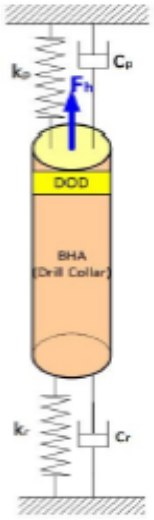

Fig. 8: Spring, Mass, Damper Model (Wang, Butt, & Yang, 2013)

Using these models together Wang et al. was able to simulate the BHA displacement and WOB when drilling with and without the DOD. Time series plots of the WOB over time are shown in Fig. 9 for the WOB profile when drilling on a flat surface with and without the DOD.

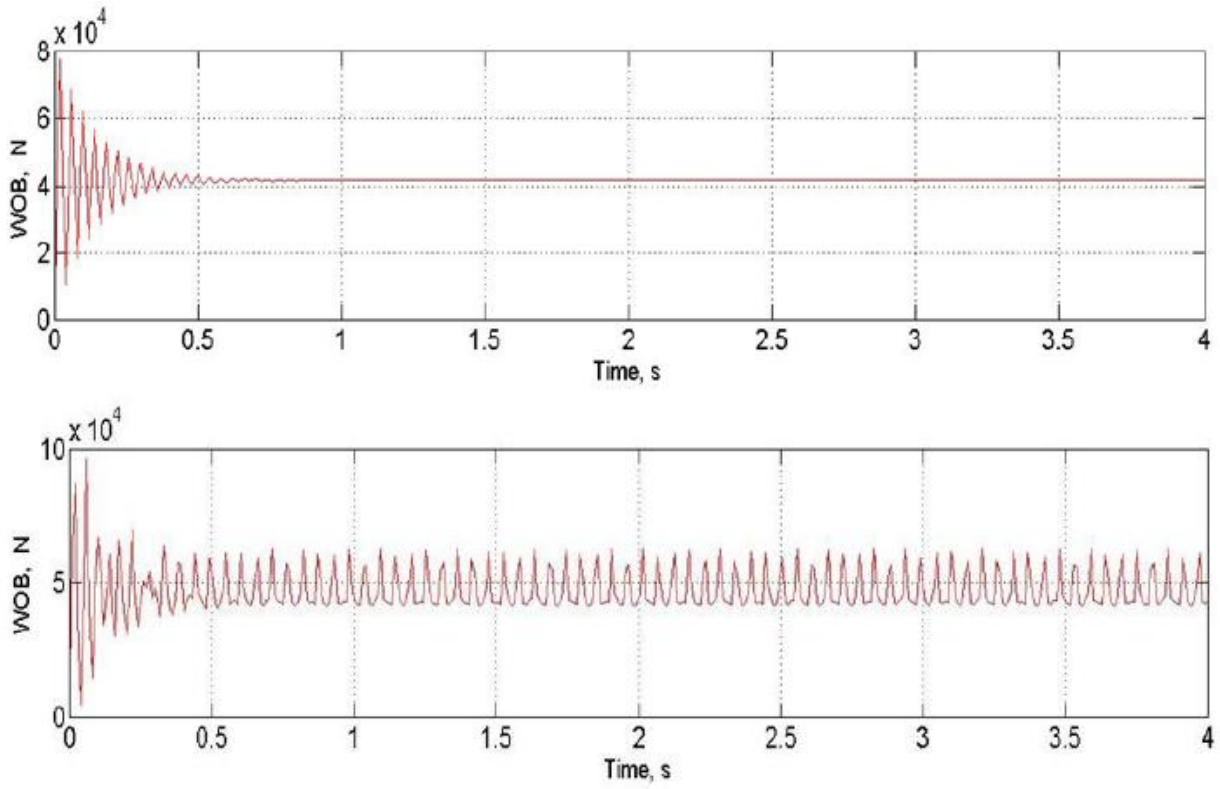

Fig. 9: WOB profile when drilling without (top) and with (bottom) the DOD (Wang, Butt, & Yang, 2013)

Wang et al. related the average ROP to the pressure pulsation amplitude of the DOD (Fig. 10) showing a small but positive increase in ROP of about 3% when the pulsation amplitude was increased by 60%. Wang et al. also mentioned that drilling fluid properties affect the enhancement provided by the DOD and that with higher density and viscosity fluid the ROP would increase by 8% (Fig. 11).

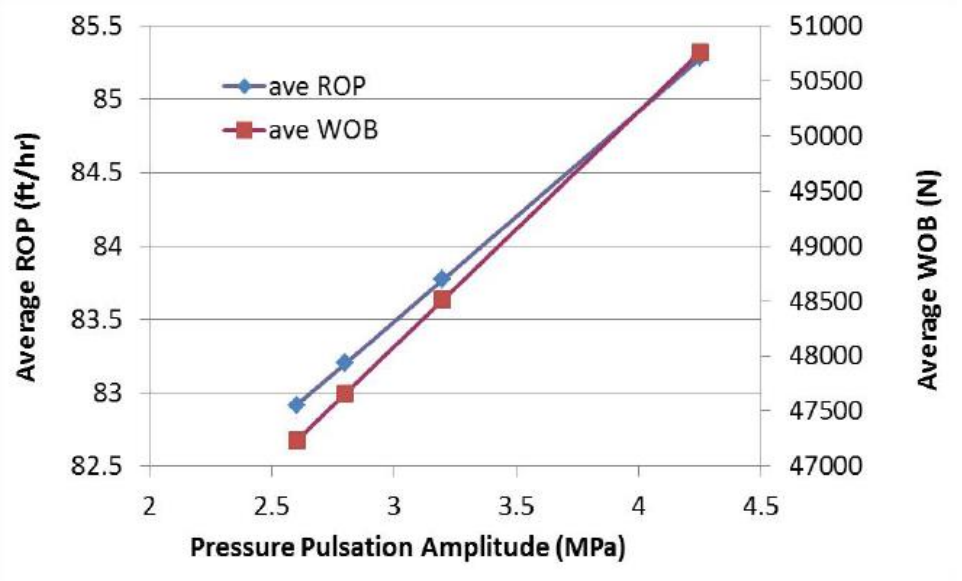

Fig. 10: Average ROP vs Pressure Pulsation Amplitude (Wang, Butt, & Yang, 2013)

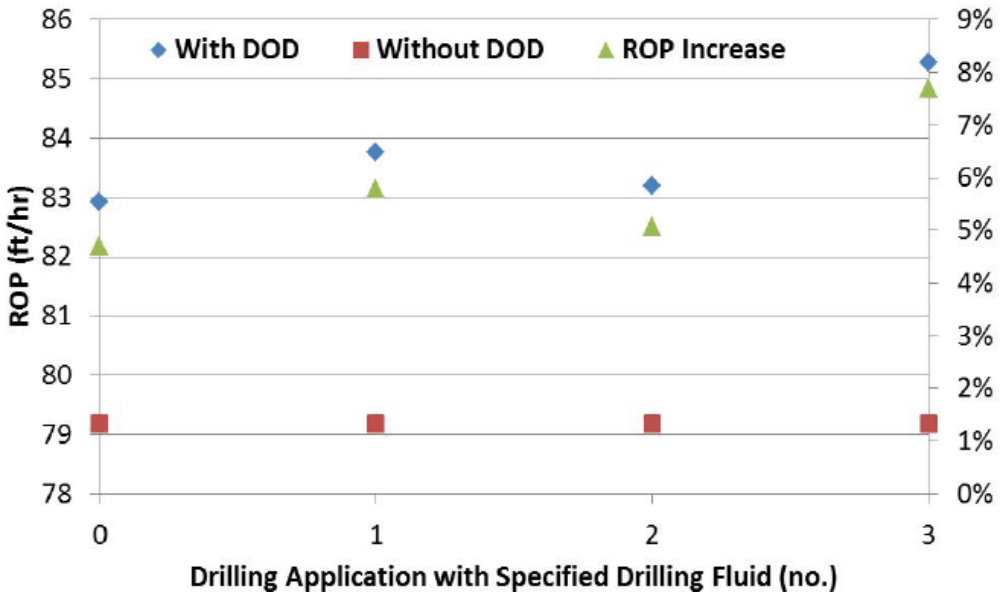

Fig. 11: ROP & Percentage increase due to different drilling fluids (Wang, Butt, & Yang, 2013)

Until this point mainly applied vibration has been reviewed. Also of interest is the idea of utilizing self exciting vibration or damping specific vibration. This is the idea of a passive vibration tool that allows the bit some axial freedom or compliance. Such a device was tested by Masoud Khademi (Khademi, 2014). Khademi's test device

consisted of a set of rubber mounts located between the drilling sample and the support frame of the laboratory drill rig. This mounting system allowed the rock sample to vibrate naturally under the bit. Khademi then varied the compliance of the mount which changed how the rock sample would vibrate.

Khademi found that there was a "sweet spot" for the compliance of his system as related to ROP. It was found that increasing the compliance resulted in an increase in ROP until the optimum point was crossed and ROP dropped (Fig. 12). Khademi related this increase in ROP back to an increase in DOC though dividing the ROP by the RPM, the results are shown in Fig. 13 and Fig. 14.

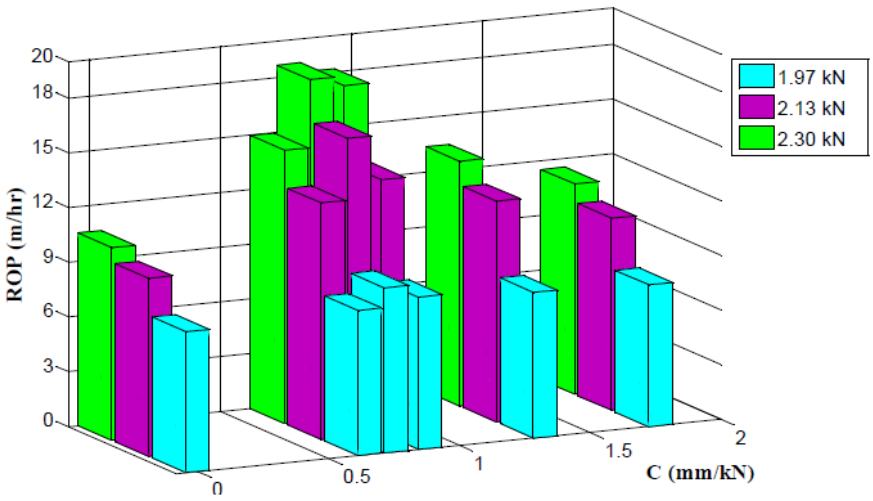

Fig. 12: Compliance vs. ROP for various WOB (Khademi, 2014)

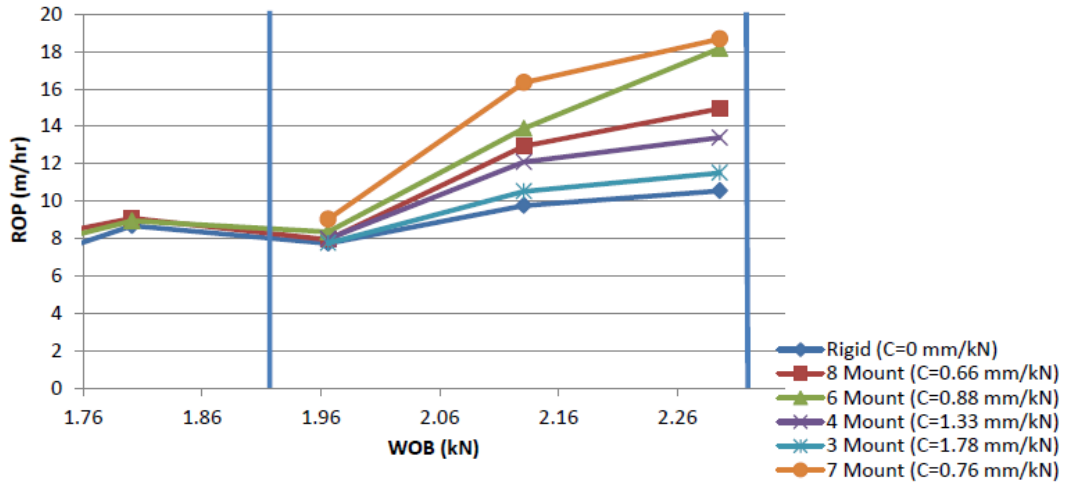

Fig. 13: ROP vs WOB for various levels of compliance (Khademi, 2014)

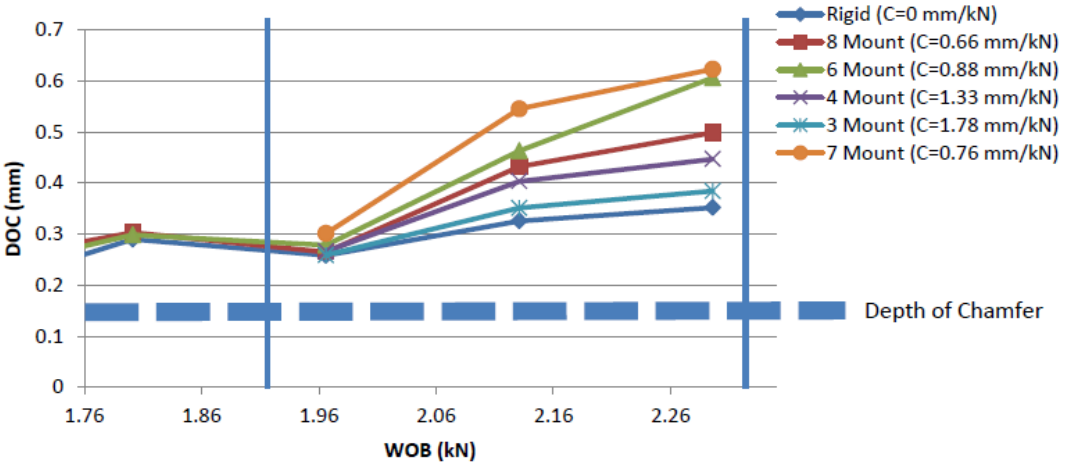

Fig. 14: DOC vs WOB for various levels of compliance (Khademi, 2014)

Because Khademi's initial results looked promising, the Drilling Technology Laboratory at Memorial designed a laboratory scale compliance tool to be mounted above the bit (Fig. 22). The tool consisted of an inline belleville spring and damper stack (Fig. 23). Results from these experiments were presented by Rana, P.S. et al (Rana, 2015).

Rana et al preformed 80 test runs, combining four levels of compliance, five levels of weight on bit and four different flow rates. The tool was tested by performing drill off tests into specially developed rock analogue specimens.

It was shown that without use of the pVARD tool, ROP was proportional to applied WOB (Fig. 15). Graphing the ROP vs WOB for multiple tool configurations at different flow rates showed the pVARD tool did increase ROP in some instances. Khademi's work suggested that there would be an optimal compliance design for specific drilling parameters. ROP vs WOB graphs of the laboratory pVARD tool can be seen in Fig. 16.

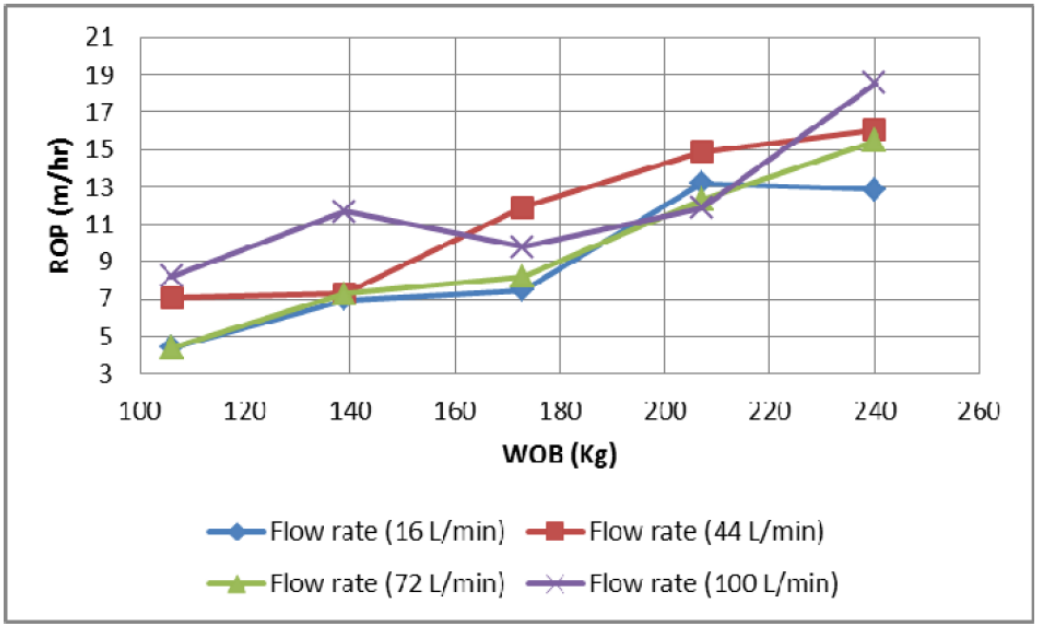

Fig. 15: ROP versus WOB for conventional drilling (Rana, 2015)

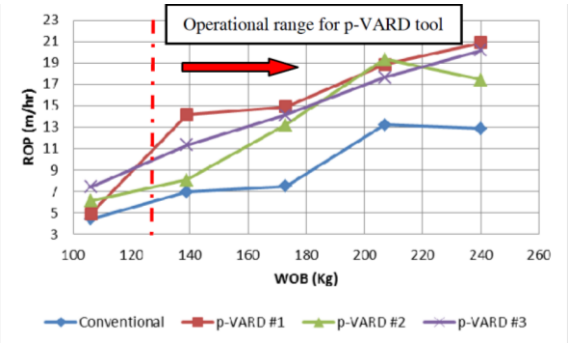

Flow Rate 16 L/min

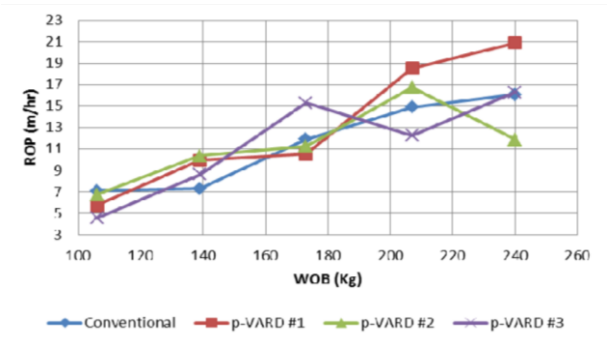

Flow Rate 44 L/min

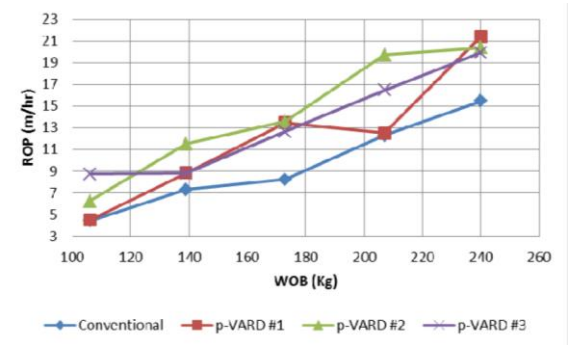

Flow Rate 72 L/min

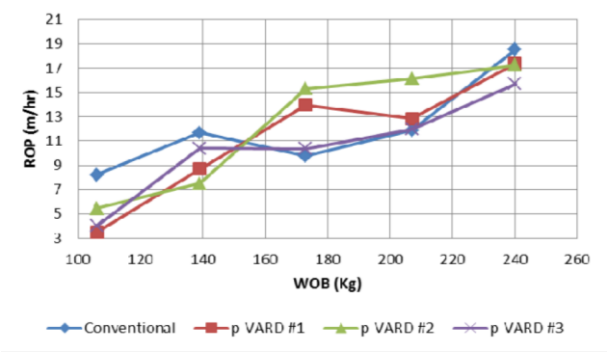

Flow Rate 100 L/min

Fig. 16: ROP versus WOB at various flow rates and compliance settings (Rana, 2015)

From this data Rana et al concluded that a pVARD tool of this design could indeed increase ROP and that such a tool would have a specific operational range. Lastly Rana et al concluded that flow rate has a significant effect on the pVARD tool performance and that the axial vibrations generated by the tool assisted cutting removal at low flow rates.

Zhong, Yang and Butt also looked at enhancing drilling penetration using passive vibration (Zhong, Yang, & Butt, 2016). They used simulations created with PFC2D and calibrated using laboratory tests with the lab scale pVARD tool discussed later in this thesis. The PFC2D model was setup with the bit axial motion having spring stiffness and a damping

coefficient (Fig. 17). They characterized their results using mechanical specific energy (MSE), depth of cut (DOC), and material removal rate (MRR).

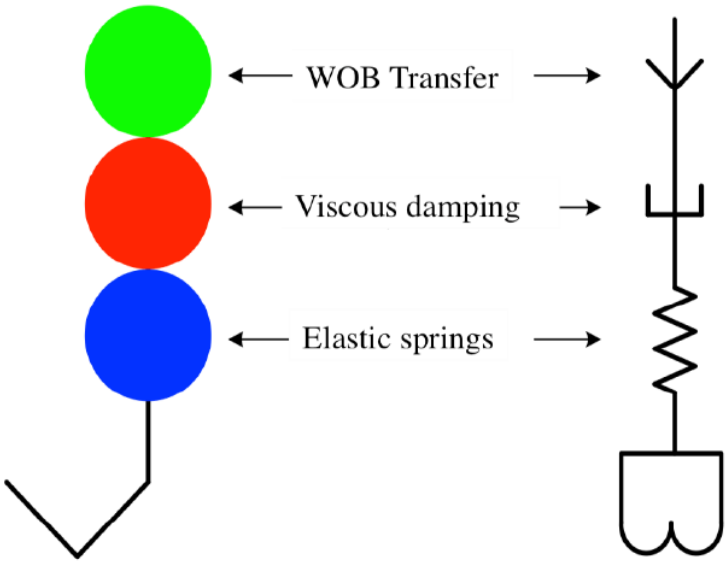

Fig. 17: PFC2D model setup for pVARD (Zhong, Yang, & Butt, 2016)

Drill off tests were performed in representative rock samples with unconfined compressive strength of 46 MPa using a 35mm, 2 cutter, PDC bit on and the laboratory scale drill rig (Fig. 22). These drill off tests were then compared to the PFC2D model outputs (Fig. 18).

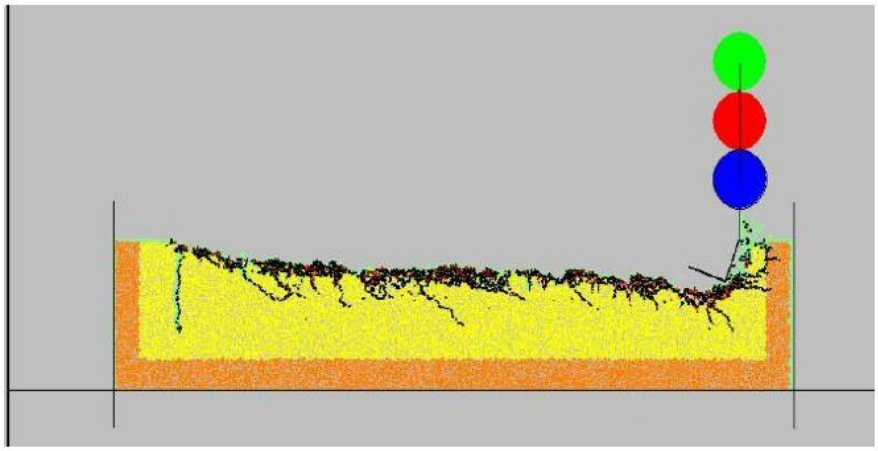

Fig. 18: Completed PFC2D Simulation (Zhong, Yang, & Butt, 2016)

Zhong et al found that the simulation results agreed with the experimental data except for the Y-axis values for mechanical specific energy. They believe the error in MSE is due to the model not being able to consider fluid flow rate. The authors also used the simulation to show the bit vibration with the use of the pVARD versus a rigid bit configuration (Fig. 19). Overall Zhong et al found that the experimental drilling setup could be simulated using discrete element modeling.

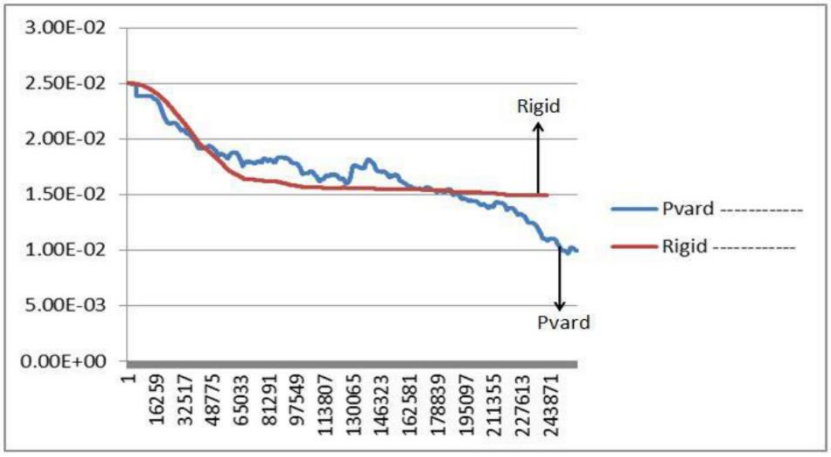

Fig. 19: Y-axis bit position from PFC2D simulations (Zhong, Yang, & Butt, 2016)

2.4 **Shock Absorbers**

Shock absorbers, or bumper subs, are a class of drilling tools that used to reduce the amount of vibration transmitted from the drill bit to the bottom hole assembly. Depending on the design of the shock absorber it may absorb just vertical vibrations or both vertical and horizontal vibrations. There is also a variety of shock absorber mechanisms from spring and damper combinations to hydraulic tools. Shock absorber manufacturers also claim that the tools increase ROP, such as Schlumberger's Shock Sub (Shock Sub Tool Increases ROP 50%, Reduces Axial Vibrions While Drilling 22-in and 16-in Sections, 2015). Manufacturers of shock tools don't explain how their tools

increase ROP past the fact that the tool reduces impact loads to the BHA. How the reduction of impact loading increases ROP is not clear as it would depend on whether it was drilling ROP or if these companies are referring to job time. It is apparent that the reduction of impact loads to other drilling tools in the drill string would increase the lifespan of these tools leading to fewer trips to surface due to tool failures. Reducing trips to surface would lead to reduced job time but not necessarily improved instantaneous ROP or depth of cut.

3 Drilling Tool Design and Prototyping

Both the lab scale pVARD tool and the field trial prototype pVARD tool were designed to investigate the mechanisms by which passive vibration affects drilling efficiency. Both tools allow their mechanical parameters, spring rate and dampening, to be adjusted through rearranging of the tools internals. The design of these tools is covered in the following sections.

3.1 **Design of the lab scale pVARD Tool**

A laboratory scale pVARD tool (Fig. 21, Fig. 23, Fig. 24) was designed for use on the small drilling simulator (Fig. 20). The results of this tool were described earlier by Rana et al. The lab scale pVARD tool was designed with three main operating sections, these are the; motion transfer, spring, and damper sections and was constructed in a manner to allow its internal springs and dampers to be reconfigured easily. To operate with the small drilling simulator the tool was designed to work with loads up to 250 kg, torques up to 600 Nm and flowing pressures of 1,000 PSI. As the tool would be used in a laboratory environment a minimum safety factor of five was employed to ensure that the device would not be a safety risk during operation.

Fig. 20: Small Drilling Simulator

3.1.1 Motion Transfer section

This section allows rotary movement to be transferred though the tool while allowing axial movement within a defined range. This was accomplished using a keyed shaft and shell arrangement where the spring and damper sections are sandwiched between ledges in the shaft and shell as shown in Fig. 21. The top of the shaft contains the box thread to connect it to the drill string. The shaft is hollow to allow drilling fluid flow through the tool. The largest section of the shaft holds the keys that transfer rotary power to the shell. Below that are the steps for engaging the damper and the springs. At the bottom is a double O-ring stack to allow transfer of drilling fluid. These O-rings are dynamic and slide as the tool is compressed. The tool was designed with two O-rings to reduce failures while operating.

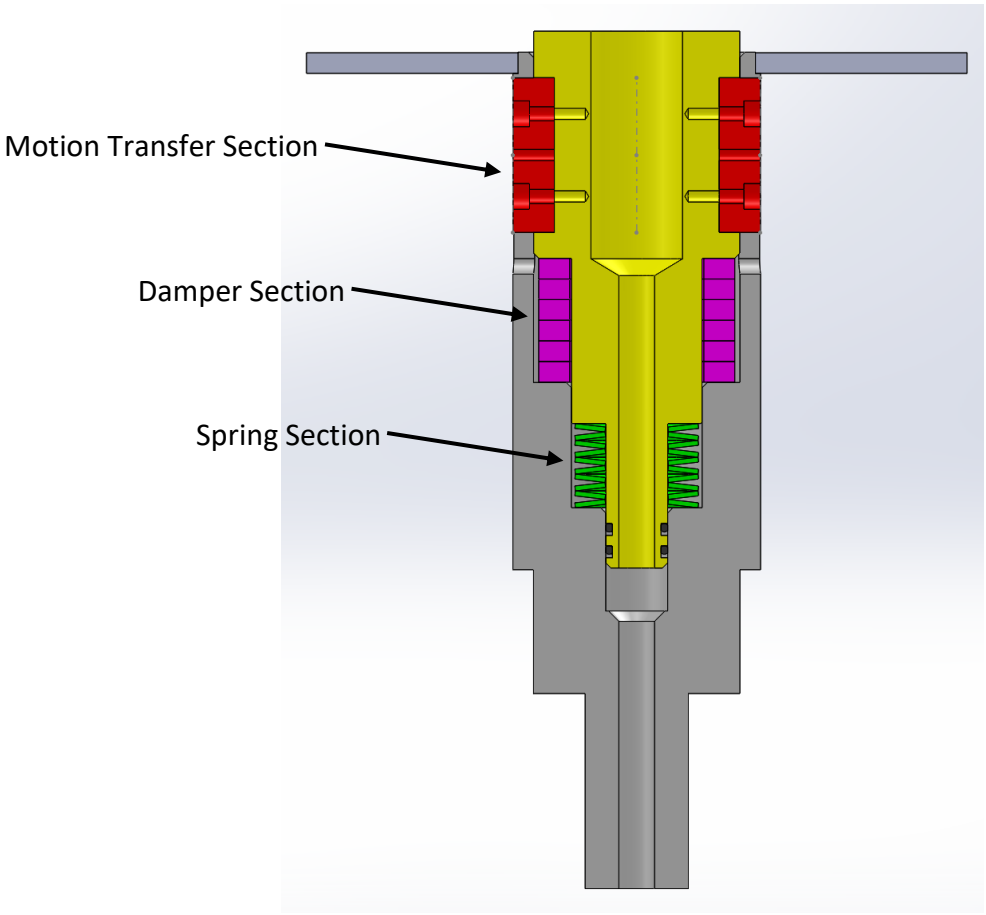

Fig. 21: Lab Scale pVARD Tool Section

The shell has mating features for the shaft. Slots for the keys and matching ledges to contain the springs and dampers.

Because the tool was going to be used in a laboratory setting, safety and ease of use were considered in the design. The shaft and shell design contain the spring and damper pieces within the tool while the key ways were designed to transfer the rotational loading through the key material while the compression loading is transferred through the spring and dampers from the shaft to the shell. This design ensures that the key fasteners are not loaded in shear. The keyways were sized to make assembly of the tool easy as

sizing them for the required load would result in extremely small components that would be difficult to handle. Sizing the keys for assembly created components that could be easily manufactured and assembled while providing plenty of safety factor for unpredicted loading scenarios. An example calculation for confirming the strength of the keys is shown in Appendix A-1.

O-Rings were chosen using Parkers O-Ring Handbook. Values for static seals were used to give higher seal compression, as the operating pressure within the tool could be as high as 1,000 PSI. In Appendix A-2 is an example of calculating the squeeze on the O-Ring to confirm that at minimum material conditions the seal will function.

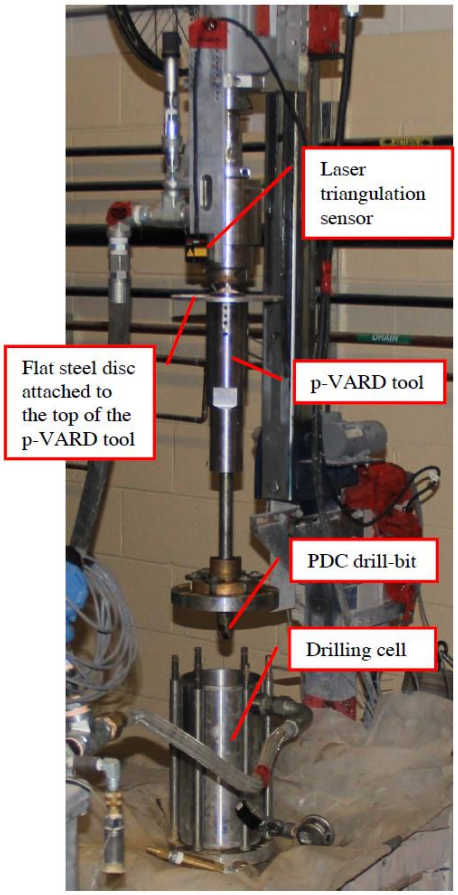

Fig. 22: Lab Scale Drilling Setup (Rana, 2015)

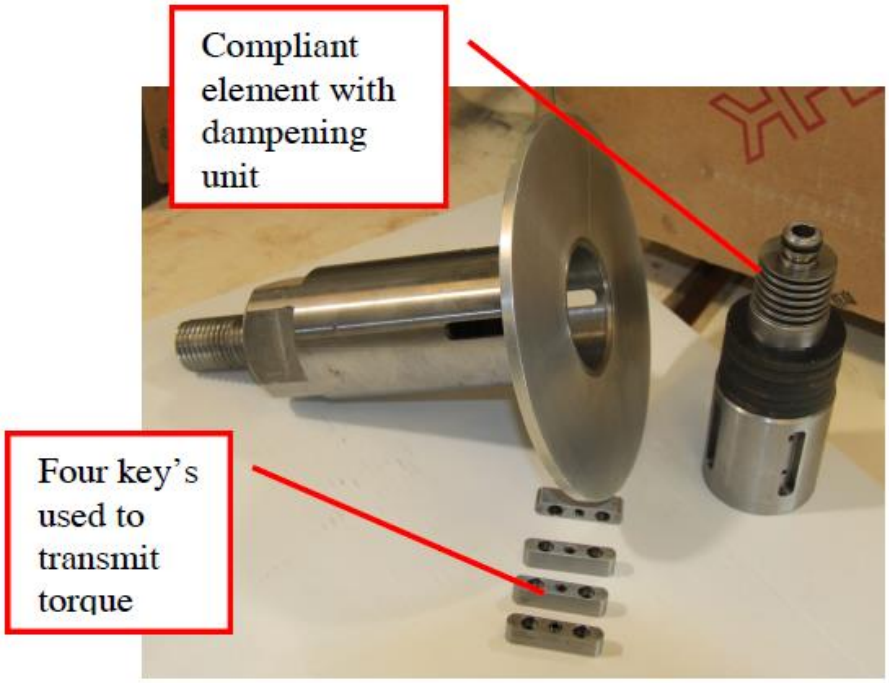

Fig. 23: Lab Scale pVARD Tool (Rana, 2015)

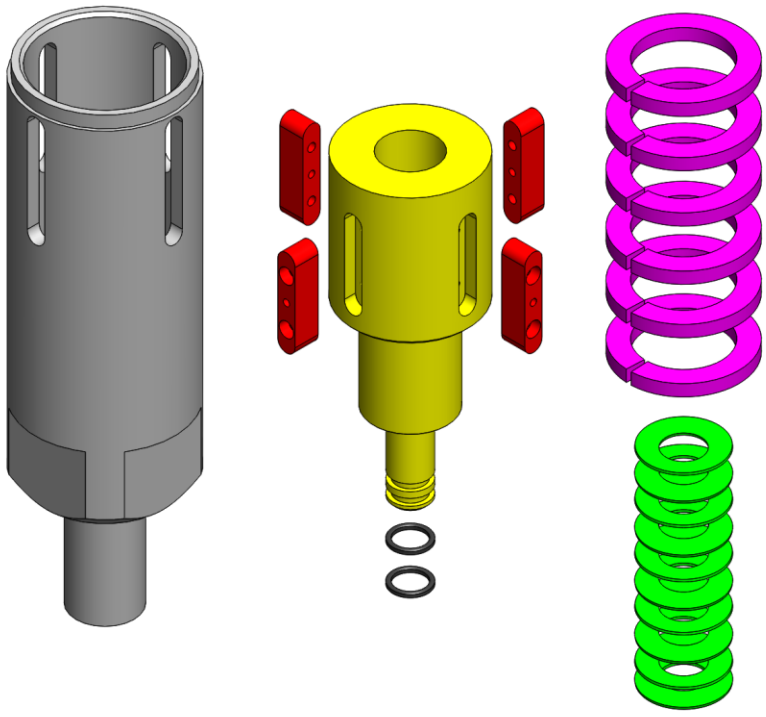

Fig. 24: Exploded View of Lab Scale pVARD Tool

3.1.2 Spring Section

The spring section consists of a stack of Belleville washers. The spring section is designed such that the washers are stacked individually in series or made into parallel stacks that are then stacked in series (Fig. 25).

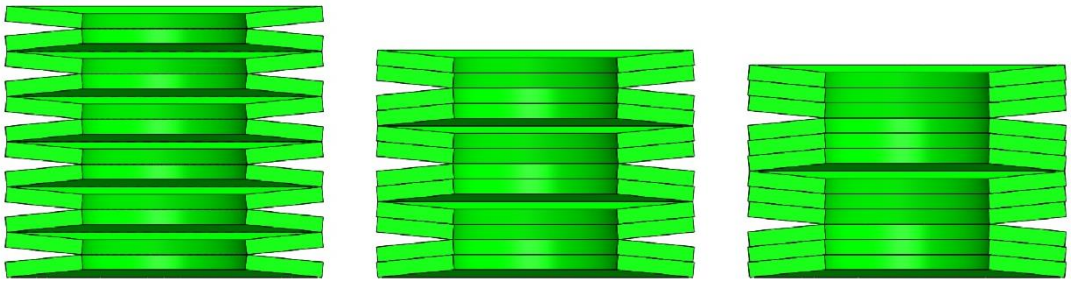

Fig. 25: Belleville Stack Patterns

Left: series stack. Center: Series stack of parallel pairs. Right: Series stack of parallel triples

These different stacking regimes allow the pVARD spring section to be setup with different spring constants while using the same washer. Parallel-series stacking is more cost efficient than buying custom springs it causes a reduction in the total travel distance of the spring stack as not as many series stacks can be fit in the same space. Appendix A-3 shows an example calculation for determining a Bellville stack spring constant. First for a simple stack of five single springs in series and second for a stack of five sets in series of two springs in parallel per set.

3.1.3 Damper Section

The damper section consisted of a stack of three rubber rings with durometer of 40A. This rubber stack was chosen as it was the softest available. The softer rubber acts

as a damper, absorbing higher frequency vibration while increasing the spring constant of the tool in compression.

Construction	Solid
Cross Section Shape	Rectangle
Material	Neoprene
Texture	Smooth
Thickness	1/4"
Thickness Tolerance	-0.031" to +0.031"
Width	12"
Width Tolerance	-0.250" to +0.250"
Length	12"
Length Tolerance	-0.25" to +0.25"
Backing Type	Plain
For Use Outdoors	Yes
Temperature Range	-20° to 212° F
Tensile Strength	1,500 psi
Color	Black
Specifications Met	ASTM D2000 BC, MIL-R-3065
Certification	Material Certification with Traceable Lot Number and Cure Date
Durometer	40A (Medium Soft)
Durometer Tolerance	-5 to +5
RoHS	Compliant

Table 1: Rubber Technical Specifications (McMater-Carr, n.d.)

3.2 Design of Prototype pVARD Tool

After building and testing the laboratory scale pVARD tool a larger design was needed to be tested in field trials. This tool would need to work with the much higher axial and torsional loads that are needed to drill rock with a six-inch PDC bit. The prototype pVARD tool would be designed in the same manner as the laboratory scale tool with the same three main sections; motion transfer, spring, and damper sections. The final

design is shown in Fig. 26 shafts are shown in yellow while the outer shell is shown in grey.

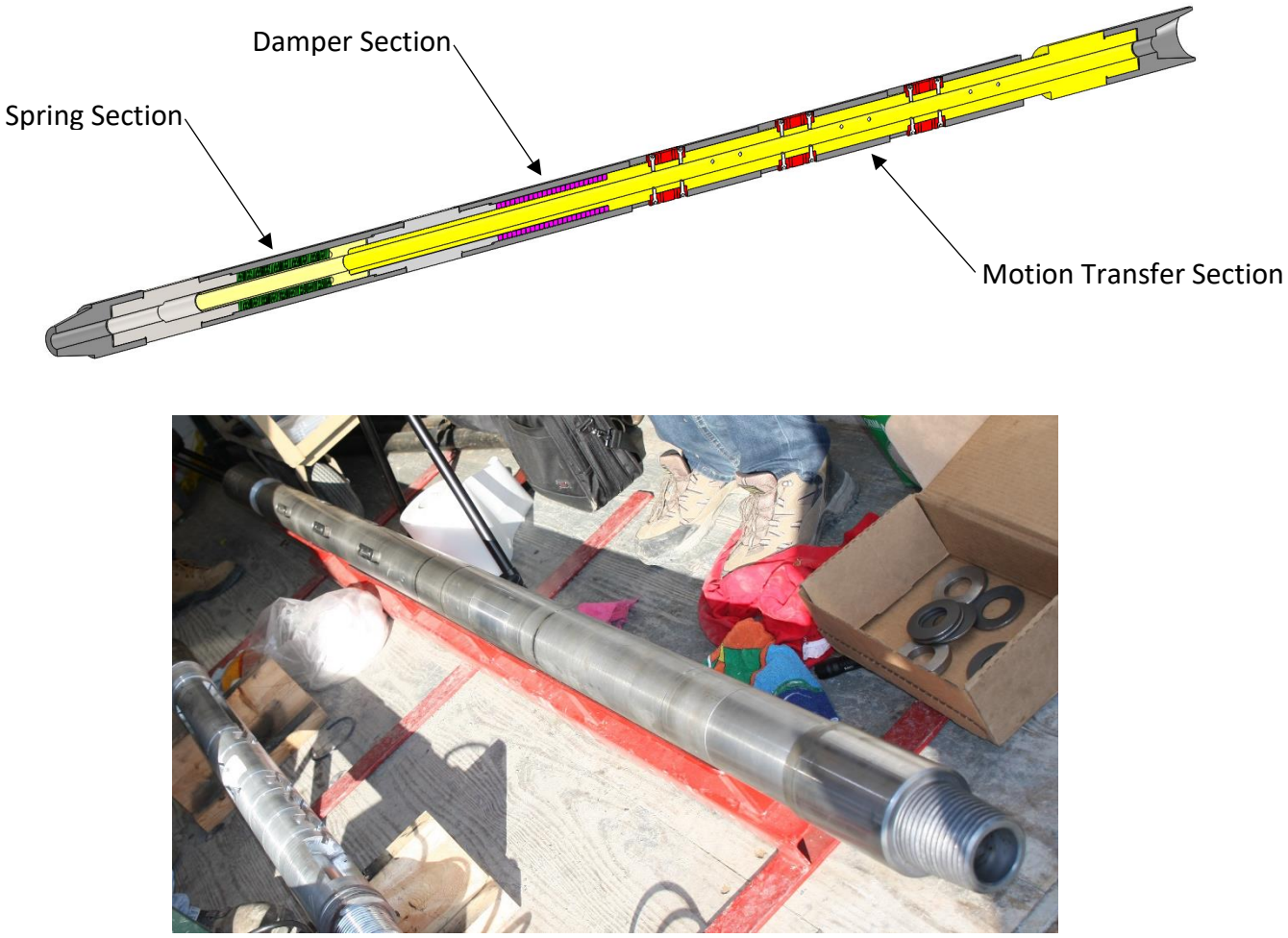

Fig. 26: pVARD Tool Section and Photo

3.2.1 Prototype Specifications

The field trial tool would be used with and Ingersoll Rand T3W drill rig that can produce 25,000 lbf downward thrust, 8,000 ft*lbf of torque, and 40,000 lbf of pull back capacity. Added to the downward thrust would be the weight of the 200-meter drill string. The tools outer diameter was limited to 4 inches as to be compatible with a bottom hole

assembly utilizing a 6-inch bit. The tool also had to have a fluid passage though the center of at least 1.25 inches to allow for drilling fluid flow.

Because the field trial tool would operate within a wellbore well away from the personnel operating it, the high safety factors of the laboratory scale tool were no longer needed. This said, there were still elements of the tool that were designed to have high safety factors to protect the tool from impact and vibration loading. The lower safety factor areas such as the thinner compression mandrels are housed within the tool. Because of this, if one of these areas were to fail, the tool would still be able to be pulled to surface and would not be lost in the well.

3.2.2 Motion Transfer Section

The motion transfer section for the field trial prototype consists for a two-part inner shaft. Unlike the lab scale tool, the Bellville washers for the field trial prototype are the same size as the damper segments. This prevents the parts from being nested on a single shaft. Because of this the springs were mounted on the lower shaft that is held within the tool by the lowest section of the outer shell. This allows the springs to be quickly accessed by unthreading the bottom section of the shell and removing the lower shaft with the springs. This was important as the springs would need to be reconfigured during the field trials and time was limited. The top section of the shaft has a straight thread to allow for the use of a cross over to the desired pipe thread. The thickest portion of the top shaft, just below the top thread, contains the key way system. A spline connection would be preferable to the keys, but it was known that manufacturing time would be an issue. It was also known that the tool would not be operating for long

periods of time so the decision was made to use key ways. The keys were sized to withstand multiple times the full torque output of the drill rig so that there would not be issues caused by impact loading while drilling. Calculations showing the loading capacity and safety factor for the keyed interface are shown in Appendix A-1. The keyed interface not only transmits the rotational power, but it also transmits the axial load when the tool is loaded in tension.

Torque is transmitted from the top shaft through the keys to the outer shell. The torsional capacity of these components needed to be checked. The calculations for the torsion of the top shaft and the shell is shown in Appendix A-5. A portion of the axial load is also transmitted through the bottom section of the top shaft. This segment is much thinner than the rest of the shaft so the stress and buckling capacity for this segment were checked. Those calculations are shown in Appendix A-6. Similar calculations were done for other sections of the shaft and shell but as this section was the weak point with the slenderest aspect ratio and the smallest cross section, the calculations for it are described in A-6.

3.2.3 Spring Section

The spring section in the prototype tool used a stack of Belleville washers from McMaster-Carr (Part 9712K478). These Belleville washers were chosen because they would allow a varied range of spring constants from a single stack of 46 washers with a spring constant of 1211 lbf/in and over 2.5 inches of travel, to a series stack of 20 sets of 3 washers in parallel. The series parallel stack had an overall spring constant 8,357 lbf/in

and a total travel of just over one inch. Example calculations for the spring constants in the pVARD prototype are shown in Appendix A-7.

These washers were also chosen for their dimensions, as the tool required an overall outer diameter of four inches and a minimum inner diameter of 1.25 inches. These washers had a large enough inner diameter that allowed the hollow lower shaft of the motion transfer section to pass though while having an outer diameter that would fit within the outer shell without needing to enlarge the outer diameter of the tool past four inches.

3.2.4 Damper Section

The damper section of the prototype tool was also built in the same manner as the laboratory scale tool. The same 40A durometer rubber was used, but in a much longer stack to achieve the longer stroke of the prototype tool. In total, 24 rings of half-inch thick rubber were used to create the damper section of the tool.

3.3 **Next Generation pVARD Tool**

The lessons learned (section 6) from designing the first field trail prototype of the pVARD tool will be used to create the next generation pVARD tool. The tool will be made stronger and more compact using better materials and “design knowledge” gained from building and trialing the first prototype.

4 Field Trials of pVARD

4.1 **Field Trial Summary**

During the field trials multiple tests had to be accomplished in a short amount of time. Due to the cost of renting a drill rig, the testing time was limited to 7 days, September 1st through the 8th, 2014. During this time experiments related to bit wear, drill string vibrations, and the pVARD tool were conducted. A total of three, approximately 400 foot deep, wells were drilled with the rented Ingersoll Rand T3W drill rig (Fig. 27) using different combinations of tools. The drill rig had a pull down capacity, force it could apply downward, of 25,000 lbf, while its rotary table could produce 5,500 ft-lbs of torque at 145 RPM.

Fig. 27: Ingersoll Rand T3W onsite during field trials

In the planning phases of the field trials geological records were examined for multiple locations across the Avalon peninsula in eastern Newfound Land. A site was chosen in a quarry on Red Bridge Road in Conception Bay South (Fig. 28). This site was chosen as it had consistent layers of Grey and Red Shale (Fig. 29) with Unconfined compressive strengths of 61 and 56 MPa respectively (Reyes, Kyzym, Rana, Molgaard, & Butt, 2015).

Fig. 28: Field Trial Location, Conception Bay South

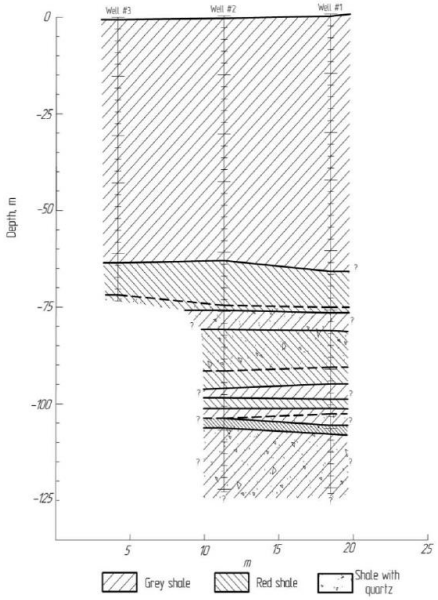

Fig. 29: Geological cross-section of field trial site (Reyes, Kyzym, Rana, Molgaard, & Butt, 2015)

Test runs were staged such that multiple tool configurations could be tested in similar rock formations. To accomplish this the rig would perform a drill off test by drilling a short segment of the well with a given WOB while recording the ROP and holding other drilling parameters constant. The WOB would then be increased and the test repeated. After the drill off test was completed the tool string was removed from the hole to change the tool configuration. The string would then be put back down the well to perform another drill off test. By understanding the lithology and looking at the returned cuttings, tests could be placed in similar rock formations allowing for improved comparison between tests. For example, while testing the pVARD tool in a grey granite rock formation the BHA was run without the tool for one drill off test and with the tool for two tests, changing the tools configuration between drill off tests. When the well transitioned from grey to red granite the BHA was reconfigured without the tool to create a base line for that rock formation and then with the pVARD tool. Having runs without the pVARD tool in each of the rock formations allowed for comparisons to be made between the drilling performance with and without the pVARD tool as well as performance to be related across rock formations by comparing the baseline tests.

4.2 Drill Bits

Three different types of bits were used during the field trials; a thermally stable diamond or TSP bit, a milled tri-cone roller cone bit (RC), and a polycrystalline diamond compact bit or PDC bit. The PDC was the main bit of interest for the field trial involving the pVARD tool. While the TSP bit was only run a few times with and without the pVARD tool. These were to be used as comparison against the PDC bit. The roller cone

bit was used in conjunction with an accelerometer sensor sub and stabilizer to experiment with drill string vibrations as discussed in section 2.3.1. See Fig. 30 for images of the PDC and roller cone bits.

PDC Drill Bit

Roller Cone Bit

Fig. 30: Drill Bits Used in Field Trials

4.3 **Bottom Hole Assembly**

A number on different components were available to be included in the bottom hole assembly, or BHA, for the field trials. For testing of vibrations both in the drill sting and at the bit, there was an accelerometer sensor sub. This sub had several accelerometers and direction measurement instruments to enable measurement of tri-axial acceleration. There was a fined stabilizer for use in drill string vibration experiments. There were the three types of drill bits described in the previous section and the pVARD prototype tool itself.

4.4 Surface Data Collection

During the field trials as much data was collected as possible. Because the drill rig had only analog instrumentation and no data recording system, data for each run was collected and entered manually. For each run a start and end time was recorded along with; penetration depth, feed pressure, total string length, fluid flow rate, and drill string rotation rate (RPM). With these data points the normalized rate of penetration and the weight on bit (WOB) could be calculated for each experimental run. This normalized rate of penetration, which can be described as the penetration per revolution of the bit, allows for comparison of ROP across varying drilling parameters. As the rig had no measurement for torque on bit, this value was estimated using the available data and the equation for torque on bit,

$$T = \frac{1}{3} * WOB * D_{bit} * Friction\ Factor$$

Where D_{bit} is the diameter of the bit, WOB is the weight on bit. This calculation for torque then allowed the calculation of mechanical specific energy.

4.5 Downhole Data Collection

During some of the trials, specifically those looking into drill string vibration while drilling with a roller cone bit, a downhole sensor sub (Fig. 31) was used to measure acceleration of the bottom hole assembly. This device was developed by the Drilling Technology Laboratory specifically for these field trials and utilized a custom electronics system within a non-magnetic body. Three accelerometers and a magnetometer measure vibration in all axis' while rotating. This electronics package is shown in Fig. 32.

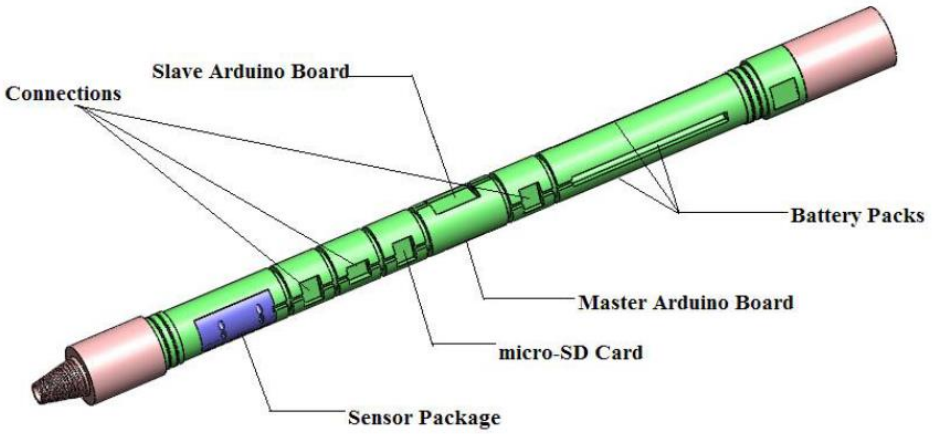

Fig. 31: DTL Downhole sensor (Gao, 2015)

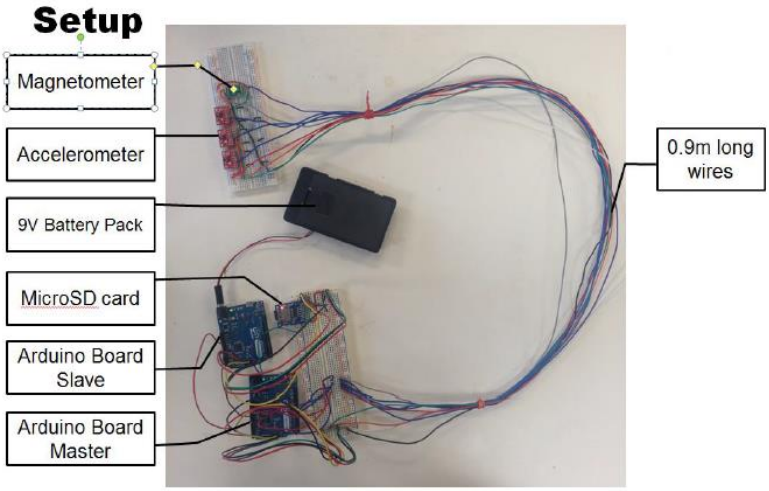

Fig. 32: Downhole sensor electronics package (Gao, 2015)

5 Results

5.1 **Lab Scale Results**

Table 2 shows the results from 80 drilling tests using the lab scale tool. The measured values for WOB, RPM, ROP, and the drill output torque are used to calculate the mechanical specific energy (MSE) for each test run. The calculation for MSE is described in section 2.1. These values are shown in italics in Table 2, and are graphed in Fig. 33 to Fig. 36. For these test runs the lab scale tool was configured with three different spring constants. A set of runs was also completed with out the tool in the system, this is the "Conventional" Case.

The three different spring constants were made using two strengths of Belleville springs from McMaster-Carr. The specifications of these springs are shown in the below in Table 3 from a DTL internal report (Xiao, Abugharara, & Butt, 2019). The "pVARD 1" configuration was created by stacking 11 of the "Lab scale-soft spring" in series. The "pVARD 2" consisted of 9 of the "Lab scale-stiff spring" in series. Finally, the "pVARD 3" configuration was created using 12 of the "Lab scale-stiff spring", these 12 springs were arranged with six groups of springs in series, each group consisting of 2 springs in parallel. The resultant spring constants can be found in Table 4.

	WOB (Kg)	Flow Rate (l/min)			
		16	44	72	100
Conventional	106	*137.7*	*85.6*	*138.0*	*73.8*
	139	*114.4*	*109.2*	*108.7*	*68.1*
	173	*132.4*	*83.2*	*120.5*	*101.3*
	207	*89.8*	*79.7*	*96.4*	*99.8*
	240	*106.9*	*85.6*	*88.8*	*74.3*
pVARD 1	106	*123.6*	*105.9*	*135.8*	*173.0*
	139	*56.2*	*80.1*	*90.0*	*91.5*
	173	*66.6*	*94.3*	*73.7*	*71.0*
	207	*62.9*	*64.1*	*94.8*	*92.3*
	240	*66.0*	*65.9*	*64.3*	*79.3*
pVARD 2	106	*98.9*	*90.2*	*97.1*	*111.2*
	139	*98.3*	*76.9*	*69.3*	*106.0*
	173	*75.0*	*87.9*	*73.0*	*64.7*
	207	*61.4*	*70.8*	*60.2*	*73.5*
	240	*78.9*	*115.8*	*67.5*	*79.8*
pVARD 3	106	*81.9*	*133.1*	*69.6*	*151.0*
	139	*70.3*	*92.3*	*90.5*	*76.4*
	173	*70.0*	*64.8*	*78.2*	*95.6*
	207	*67.3*	*96.8*	*72.0*	*99.1*
	240	*68.3*	*84.5*	*69.1*	*87.6*

MSE (KSI)

Table 2: Lab scale test results

Spring Specs	Spring type and model number		
	Lab scale-soft spring	Lab scale-stiff spring	Field scale spring
Model #	9712K86	971K27	9712k478
ID (in)	0.755	0.755	1.531
OD (in)	1.5	1.5	3
Thickness (in)	0.045	0.06	0.143
Height (in)	0.093	0.102	0.213
Deflection @ working load, inch	0.024	0.021	0.056
Working Load (lbs)	283	455	3120
Flat (Maximum) Load (lbs)	400	774	4380
Material	High-Carbon Steel	High-Carbon Steel	High-Carbon Steel

Table 3: DTL spring specs (Xiao, Abugharara, & Butt, 2019)

Spring Assembly	**Spring Constant**
pVARD 1	1,225 lbf/in (215 N/mm)
pVARD 2	2,407 lbf/in (422 N/mm)
pVARD 3	7,222 lbf/in (1,265 N/mm)

Table 4: Spring constants for lab scale pVARD tool

Testing the lab scale pVARD tool on the small drilling simulator the WOB is measured by a load cell on which the sample rock is mounted. The RPM of the bit was measured using a laser sensor pointed at an engraved disc connected to the drill shaft. For every rotation three pulses were recorded by the sensor and the RPM could be measured. The average RPM for all the test runs was measured at 280. The ROP was determined by using a displacement sensor mounted on the drill rig that measures the displacement of the carriage on which the drill is mounted.

To understand the spring deflections under the various WOB's the WOB can be divided by the spring constant to give the static deflection of the tool (Table 5).

	Static tool deflection at WOB per spring setup		
WOB (Kg)	pVARD 1 (in)	pVARD 2 (in)	pVARD 3 (in)
106	0.191	0.097	0.032
139	0.250	0.17	0.042
173	0.311	0.158	0.053
207	0.373	0.190	0.063
240	0.432	0.220	0.073
Flat load deflection	0.528	0.378	0.252

Table 5: Static pVARD tool deflection at WOB

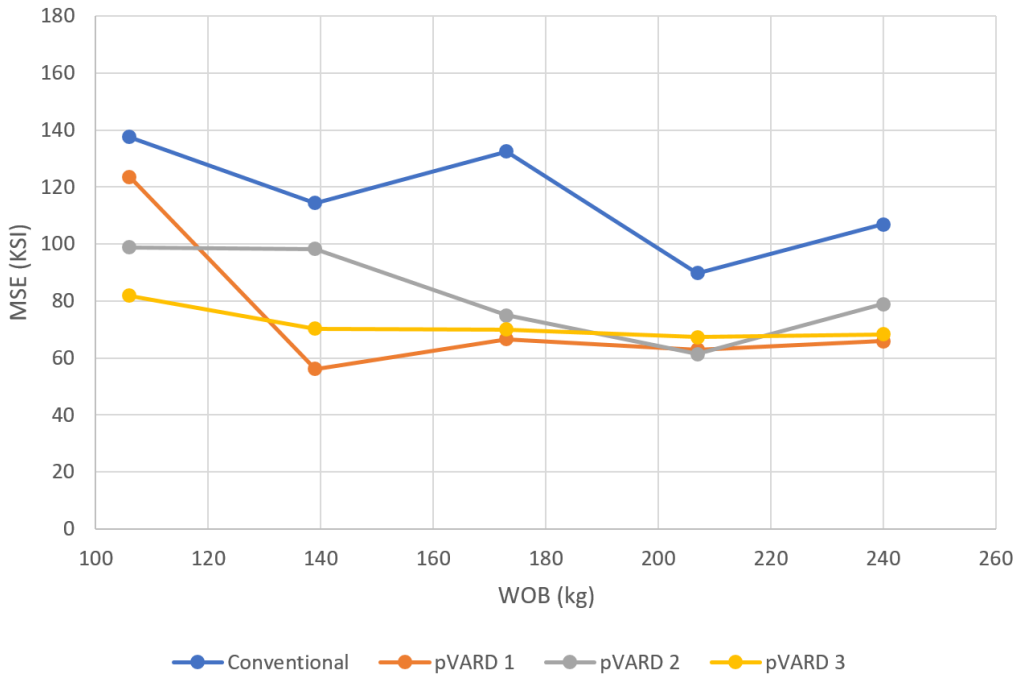

Fig. 33: Lab scale test at 16 lpm

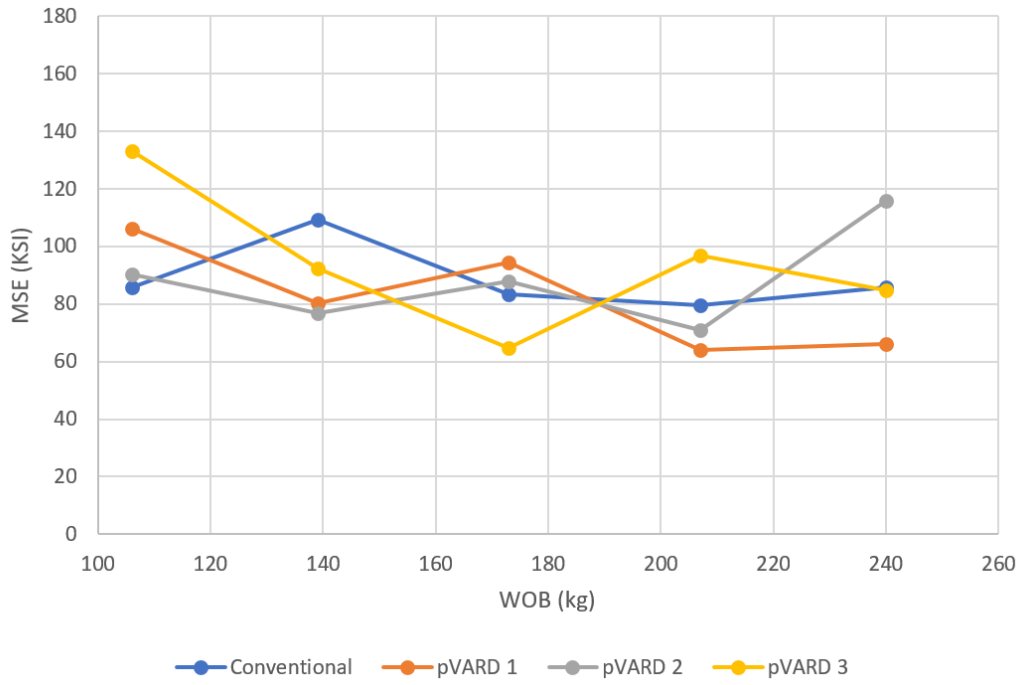

Fig. 34: Lab scale test at 44 lpm

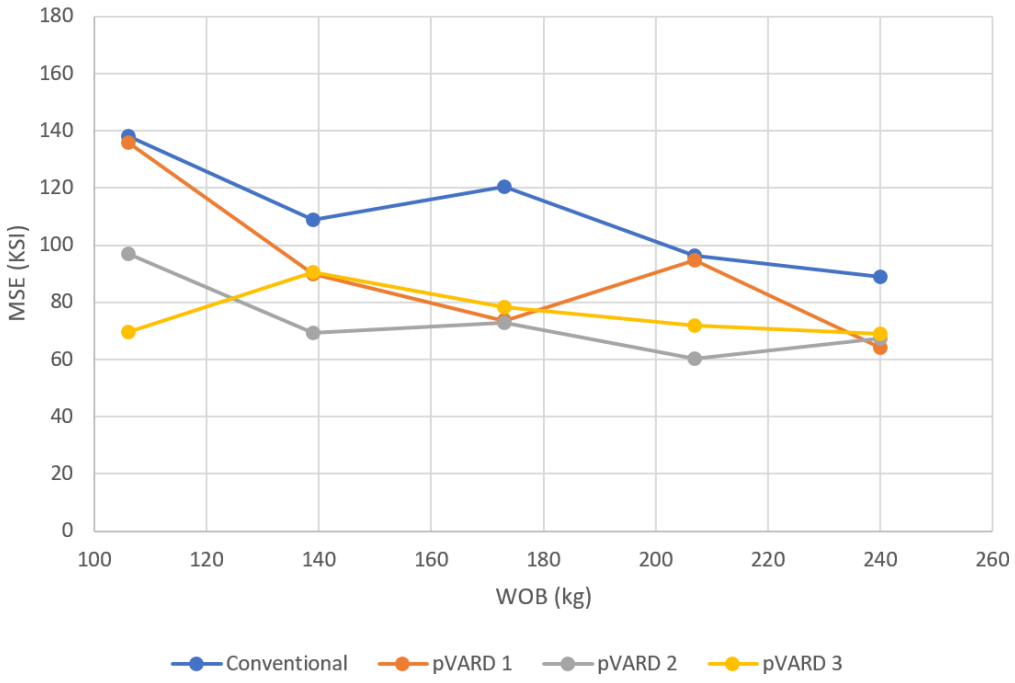

Fig. 35: Lab scale test at 72 lpm

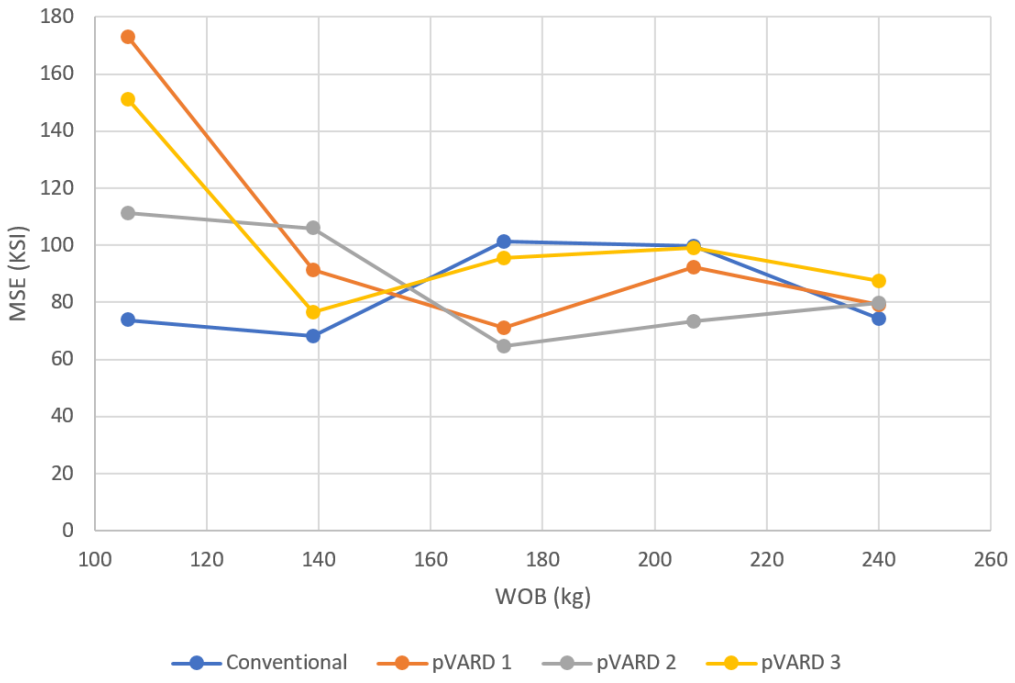

Fig. 36: Lab scale test at 100 lpm

5.2 Field Trail Results

A total of 136 test runs were conducted during the DTLs field trial, 57 of these results are presented in this thesis. The reason specific results are not included is due to them using different bits, being in different formations, and other instances that make them unsuitable for comparison. These results are all at approximately the same flow rate, 57.5 gallons per minute. The results for calculated MSE are presented in Fig. 37 to Fig. 39.

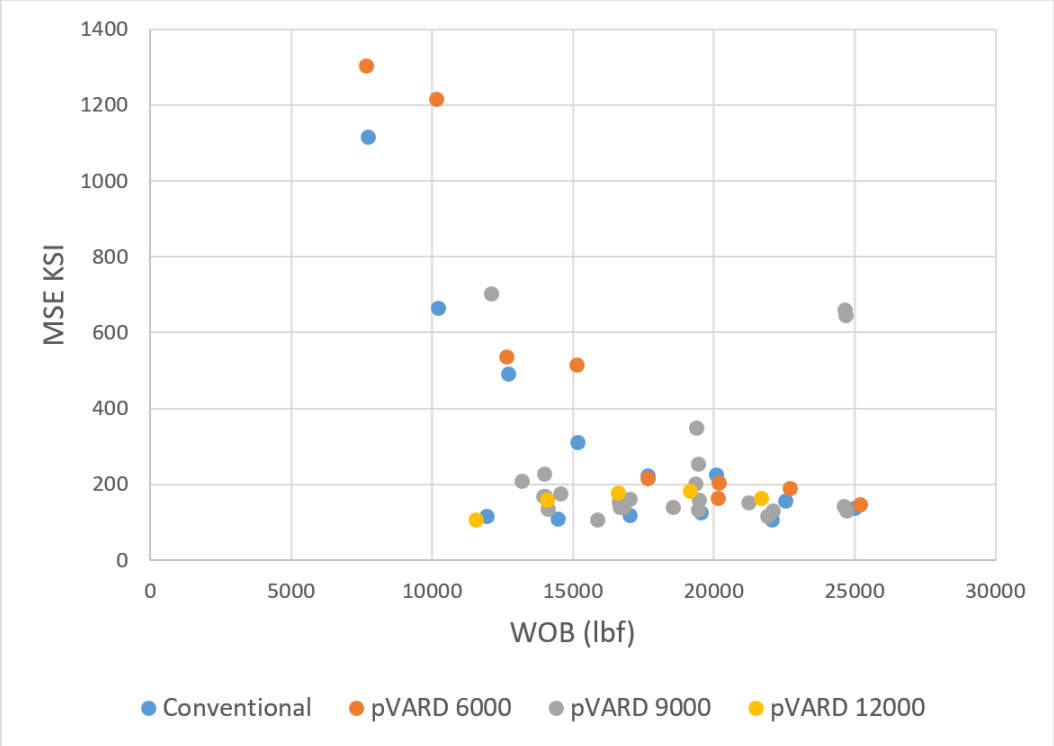

Fig. 37: Field trail results

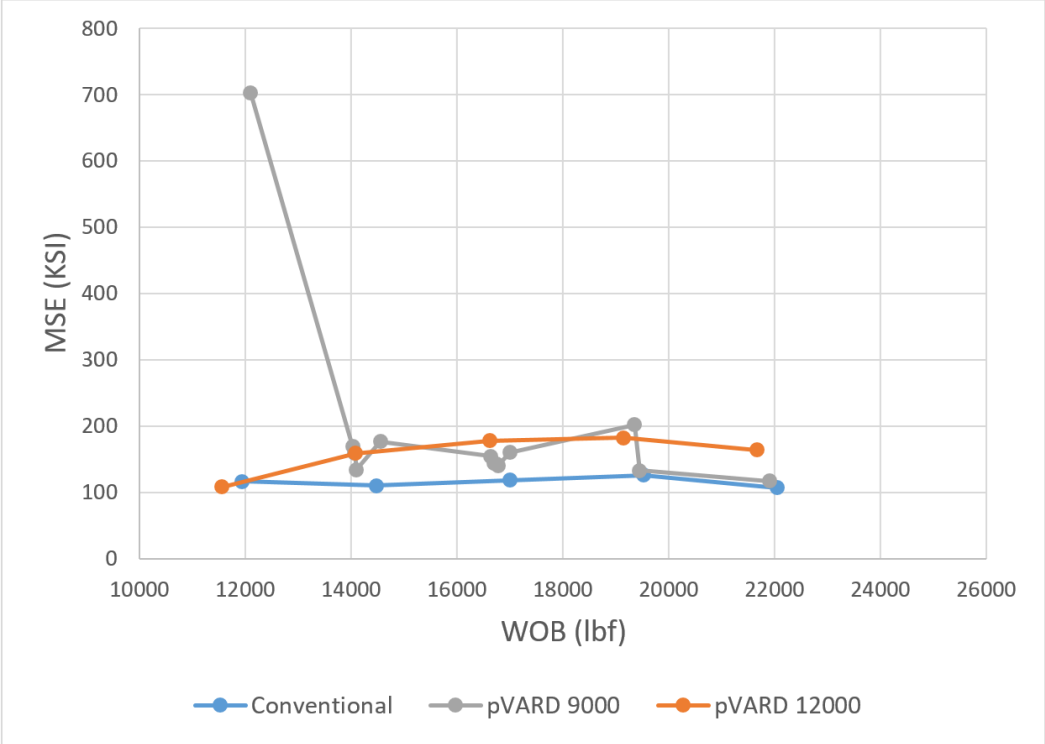

Fig. 38: Field trial tests in grey shale

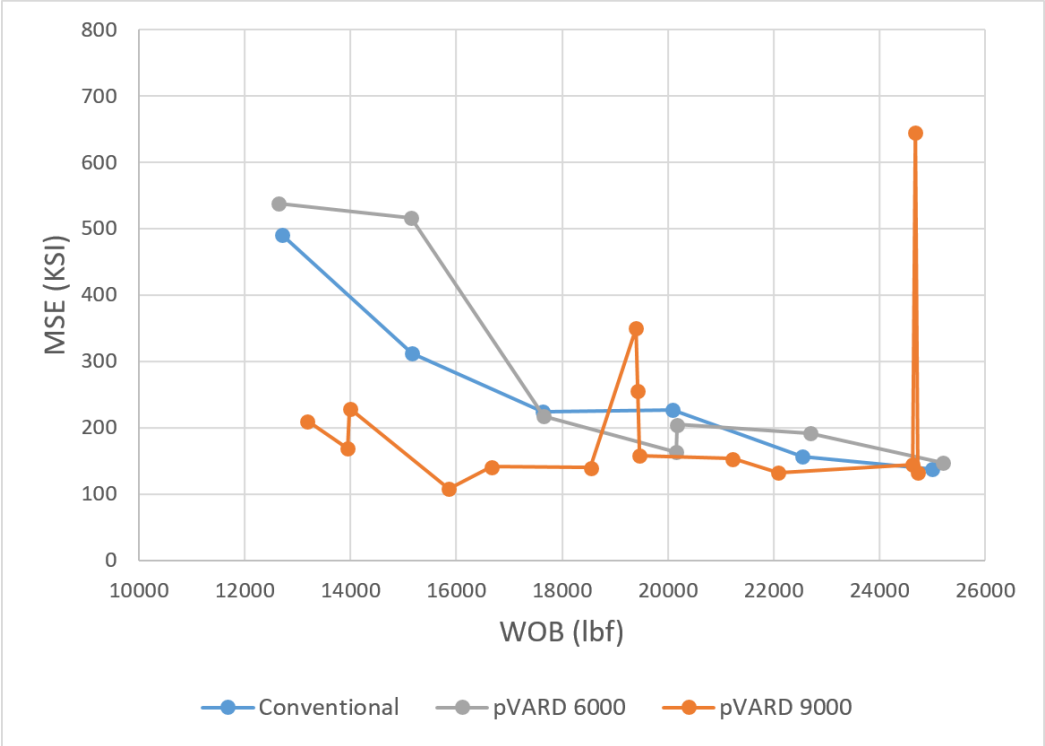

Fig. 39: Field trial test in red shale

5.3 Discussion: Testing Results

5.3.1 MSE Comparison

Looking at the calculated MSE data for the laboratory tests and comparing it to the base line conventional data in each graph we can see that for flow rates of 44 and 100 lpm (Fig. 34 & Fig. 36) the results of pVARD tool use are mixed. Sometimes the MSE is lower for the pVARD tool and others it is not. For flow rates of 16 and 72 lpm (Fig. 33 & Fig. 35) the pVARD has lower MSE across all WOB values. This seems to indicate that the impact of the pVARD tool is related to the flow rate of the drilling fluid and would suggest that the tool affects the washing of the drill bit.

Looking specifically at the pVARD 2 configuration at 72 lpm (Fig. 35), it appears that this configuration is well suited to this set of test variables as the MSE for the pVARD 2 follows the MSE for the conventional base line, holding a near constant reduction. Meanwhile examining the pVARD 3 configuration at 100 lpm (Fig. 36) seems to show the tool being mismatched with the drilling parameters resulting in mostly higher MSE values than the base line.

This appears to also be the case with most of the field trial data (Fig. 38, Fig. 39). The largest improvements in MSE for the field trial tests was seen by the pVARD 9000 configuration while drilling in red shale (Fig. 39). Most of this data showed at least a moderate reduction in MSE over the conventional baseline. None of the field trial runs seem to show any strong correlation between the pVARD and the conventional data, suggesting that the field scale tool was not “in tune” with the drilling parameters. For instance, in the test runs conducted in grey shale (Fig. 38) there is only one pVARD configuration that performs better than the conventional baseline.

Rearranging the data to compare MSE versus spring constant the effect of the tool's compliance can be seen on MSE (Fig. 40). The graph in Fig. 40 shows the MSE versus spring constant curves for the tests completed at 72 lpm at each weight on bit increment. The data points for the conventional, or no compliance, state are shown at a value of 10,000 lbf/in to aid in condensing the chart. For every WOB increment there is a spring constant that yields a lower MSE than the conventional drilling option. This suggests that the pVARD tool can in fact reduce the amount of energy required to drill a unit of volume rock.

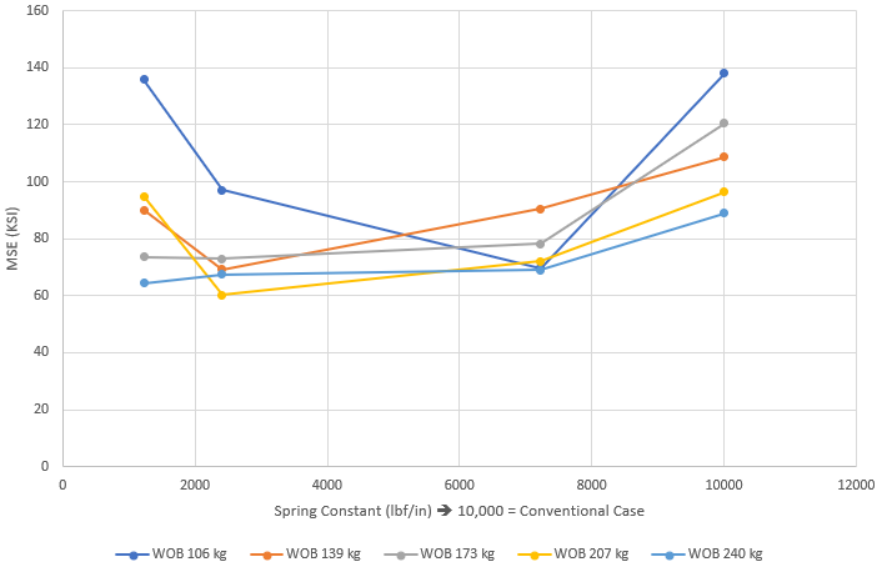

Fig. 40: MSE vs Spring Constant at 72 lpm

5.4 **Discussion: Future research**

Though this data does show instances where the pVARD does reduce the mechanical specific energy of the drilling process, a defined relationship between the operational variables and this reduction has yet to be determined.

Future research should aim to better understand how MSE is affected over a different range of variables. For instance, the current work was conducted with three compliance settings. Increasing the variety of spring constants in the test matrix could yield further clues into the tuning of the pVARD tool.

In future research it may be worthwhile to experiment with the variables that in this work were kept constant such as the RPM and the rock properties. It maybe worth trading flow rate or WOB for varied rotation speeds and compliance setting in future experimental plans. Varying RPM seems especially important as rotational speed is a key contributor to bit vibration and therefore the driving force of the pVARD tool.

6 Discussion: pVARD Tool Improvements

Throughout the development and testing process for the prototype pVARD tool future improvements were noted. Some of these improvements were left out of the original design to allow for faster development and some were discovered while assembling and using the tool. A few suggested changes came from discussing best design practices with industry experts. Including these changes in the next design of the pVARD tool would allow the tool to be shrunk in length, made easier to assemble, and be made operationally more consistent.

6.1 **Mechanical Issues with Field Trial Tool**

6.1.1 Key Bolt Failure

During the field trials the pVARD tool was used for drilling for about 3 hours and 15 minutes. During this time the only failure that occurred was in the key system used to transfer rotary power. One of the two bolts used to hold in one of the 12 keys snapped and was lost down hole. One of these keys is shown in Fig. 41.

6.1.2 Sealing Failure on Sensor Sub

The sensor sub was a second piece of equipment built by the Drilling Technology Laboratory for use during the field trials. The sensor sub contained a battery powered recording system with multiple accelerometer measurements as well as a compass measurement. This tool was used to record vibration amplitudes during some of the tests. The tool functioned until on the seals failed on the atmospheric chamber allowing fluid to

enter the chamber. The fluid pushed debris past the seal and between the metal surfaces. This made disassembling the sensor sub very difficult and caused damage to the metal parts (Fig. 42). The fluid also soaked the electronics package (Fig. 43).

Fig. 41: 1 of 12 Keys in the pVARD

Fig. 42: Sensor Sub seal Failure

Fig. 43: Electronics Package After Seal Failure

6.2 Inter-shaft connections

The shaft in the prototype pVARD tool consisted of two segments which interacted with each other though compressive contact, with the weight of the BHA

pressing the top shaft into the bottom, depending on the situation when the tool is put into tension the shaft segments could be separated. This ability to separate was designed into the tool to ease the removal of the spring section for reconfiguration. This issue with this is that without these shaft segments being rigidly connected; impact loads on these shafts can be created. Also because of the geometry of the components, these impact loads are generated on the thinnest portion of upper shaft. Threading the shaft components together allows the movement of the impacting surfaces to more robust components.

6.3 Better Sealing

The prototype pVARD tool was not sealed or pressure containing. This type of design is not usable in an actual drilling environment. The next pVARD tool needs to be sealed such that pressure differential is not lost through the tool. Holding the pressure differential prevents fluid flow through the inner working of the tool. This is key to prevent debris from entering the moving components of the tool and binding them together or causing damage. The damage caused by fluid and debris infiltration was seen in the sensor sub during the field trial and was discussed in the previous section.

Sealing the tool will require both the outer housing and inner shaft of the tool to be sealed. Backed up O-ring seals made with appropriate material for the temperature that the tool will operate in will work for static connections. The tool will require dynamic seals capable of withstanding the tools vibration for sealing between the outer housing and the shaft.

It may also be prudent to oil fill the interior of the tool. This would require a pressure compensation piston but would allow all the moving parts to remain lubricated

and clean throughout operation. Pressure compensating the tool will prevent the need for atmospheric chambers, which would require the tools components to withstand higher differential pressures.

6.4 Rotary Connection

The current tool uses a set of twelve keys to allow axial motion while transmitting rotary power through the tool to the bit. This design was originally chosen for the speed at which it would allow the tool to be manufactured and field trailed. This design is not optimal for use in oil and gas drilling for several reasons.

1. As seen in the field trials, if the bolts fail that attach the keys to the shaft a key could become liberated in the well bore. This key, being made of steel, would sink to the bottom and interact with the cutting action of the bit. This would most likely cause the destruction of the drill bit and the necessity to pull the drill string from the well, an expensive operation. The liberated key would then need to be retrieved from the well requiring another round-trip in and out of the well with a magnet.
2. As the prototype design uses the keys to hold the tool together axially, if all the keys failed, the tool would split in half. This would then require a trip into the hole with a fishing device to retrieve the remainder of the BHA, as well as another trip into hole with a magnet to retrieve the keys. The drill bit would also most likely need to be replaced due to damage.

3. Lastly, it would be difficult, if not impossible to properly lubricate the keyways as they are open to the well bore fluid. The argument could be made that the well bore fluid would lubricate the keys but that would limit the use of the tool to wells with specific drilling fluids.

A better way to accomplish the transmission of rotary power, while allowing axial movement is to use an involute spline such as those described in ANSI Standard B92.1-1996. This type of spline has similar geometry to that used for involute gears. The involute geometry, as shown in Fig.44, increases the strength of the teeth by reducing stress concentrations that would exist in a parallel key spline.

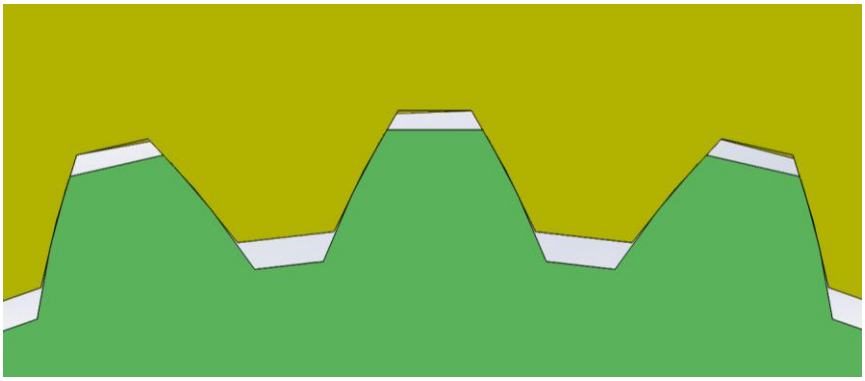

Fig. 44: Involute Gear Geometry

The use of a spline in a sealed chamber would also allow for proper lubrication allowing for increased operational life and reliability. Furthermore, I would remove the axial stopping function from the rotary joint such that the splines only see rotary force and is not the end loads created when the tool is put into tension. With the axial stop moved to another part of the tool it could be made stronger and more resilient than if it were part of the spline.

6.5 Custom Bellville springs selected for WOB application

Both the lab scale pVARD tool and the prototype tool used “off the shelf” Belleville washers as they were easy to acquire and allowed for flexibility in the tool function without the added cost of having multiple sets of springs. Making space for reconfigurable spring stacks required added length in the tool as well as caused stroke distance to change with spring rate. As spring rate went up, possible displacement when down. This is due to the parallel stacking of the springs, three Belleville washers stacked in parallel have a similar height to those stacked in series but only one third the displacement. For the next pVARD design it would be better to size the tool to specific spring rates and deflections and build custom Belleville washers to accomplish this. Custom machined Belleville springs can be made much thicker than their “off the shelf” cousins, which tend to be stamped out of thinner material. This allows for higher force carrying capacity without the need for parallel stacking. This is beneficial as parallel stacked Belleville washers have slip plains between them that add unnecessary friction into the system. Also, by custom designing the springs the geometry can be more finely adjusted to allow for better contact surfaces between the springs and the tool surfaces and between the springs themselves.

6.6 Improve interior tool joints

The prototype tool, like the laboratory scale tool uses standard “V” Threads to make up its internal connections. This was done manly for speed and simplicity of manufacturing the prototype. The next version of the pVARD tool should use Stub ACME thread geometry. Stub ACME threads are a shorter variant of the standard ACME

threads. ACME threads are a trapezoidal thread form mostly used in lead screws for their high strength. The “stub” variant of the ACME thread allows this high strength thread to be utilized in locations where connection thickness is important. This is ideal for use in downhole applications where there are tight restrictions on overall tool size.

As the stub ACME thread is not centralizing the mating parts should be designed in such a way that the thread reliefs on the end of the pin and box have a close tolerance fit to a landing surface on the mating component past the thread. This will give added bending strength to the connection by supporting both ends of the connection as shown in Fig. 45 while also centralizing the connection. The tool joint shown below also incorporates an O-Ring seal and a setscrew. The O-Ring seals the connection from flow caused by differential pressure across the connection while the setscrew is there as a backup if the connection starts unthreading due to lack of torque during assembly or reverse rotation of the tool. If the connection begins to unthread the setscrew will mechanically interfere with the threads on the pin causing the connection to stop rotating.

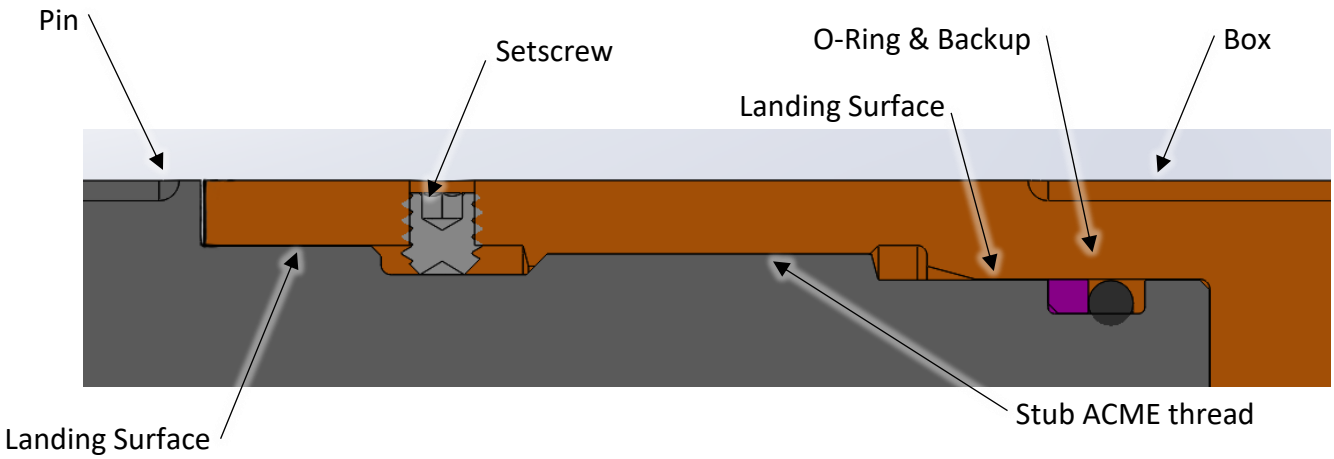

Fig. 45: Improved tool joint design

6.7 Material

The prototype tool was built mostly from plain carbon steel such as AISI 1018. This type of material has a yield strength of around 350 MPa. For prototype purposes this material good as it was readily available and easy to machine and met the strength requirements for testing. The second-generation pVARD tool will be designed for use in industrial drilling operations. As such the next pVARD tool will need to be stronger and have better ability to handle wear and erosion.

For these reasons, I would suggest that the next tool be made from 4140 HT (heat treated) or P110. P110 is a specific API steel grade where the 110 refers to its yield stress of 110,000 PSI or approximately 760 MPa. This material is more than twice as strong as the plain carbon steel and is also harder with a hardness ranging from 28 to 32 HRC. Making the tool from this material will allow for stronger more complex geometry allowing the tools size to be reduced.

After swapping the material over to 4140 HT it would also be prudent to improve the tools surfaces with further hardening. As the tool will see drilling mud containing abrasive solids flowing through it and around it, further hardening will act to prevent erosion and increase component life. Hardening will also help prevent issues such as thread galling and scratching of seal surfaces. Tool components could be gas nitrided to increase the surface hardness from around 30 HRC up to around 55 HRC. The gas nitriding is also superior to liquid nitriding as the case depth, or the depth of the increase in hardness, can be deeper. Gas nitriding can achieve depths over 10 thousandths of an inch will liquid nitriding will only penetrate about 3 thousandths.

By switching the tools material and hardening the completed components, the tools overall size can be reduced and strengthened. By improving the surface hardness, the tool will be more efficient will incur less wear-induced downtime.

7 Conclusion

To test the theory of using passive vibration to increase drilling efficiency the Drilling Technology Laboratory required prototype tools be constructed. A first prototype was designed for use with the laboratory scale drilling rig. Results from this prototype drove the development of a second prototype for use in field trials with a six-inch PDC drill bit. Through the field trials conducted with the second prototype pVARD tool several design changes were identified that would be required for this tool to be used in oil and gas drilling operations. With this information as well as the knowledge learned from the laboratory testing and field trials the next generation of pVARD tools will be designed for use in industry.

Through examining and comparing the testing results of the of the lab and field scale tools it is suggested that;

- Due to performance differences of the pVARD tool at different flow rates it appears that, the pVARD tool influences bit washing.
- As the effect of the pVARD tool on MSE varies with different drilling parameters it should be possible to tune the tool for given drilling parameters. The relationship between the drilling parameters and the performance of the pVARD tool could not be determined through the testing discussed in the current thesis.
- If the pVARD tool is incorrectly tuned for the existing drilling parameters it can increase MSE.

8 References

Ashely, D., McNary, X., & Tomlinson, J. (2001). Extending bit life with multi-axis vibration measurements. *SPE/IADC Drilling Conference.* Amsterdam, Netherlands: SPE/IADC.

Baidyuk, B. V. (1993). *Maurer Engineering (1st Ed.).* Former-USSR.

Baker Hughes. (2019, 3 7). *Baker Hughes Rig Count.* Retrieved 03 16, 2019, from http://phx.corporate-ir.net/phoenix.zhtml?c=79687&p=irol-rigcountsintl

Barkap, D. D. (1957). *Maurer Engineering (1st Ed.).* Former-USSR.

Eskin, M. M. (1995). *Maurer Engineering (1st Ed.).* Former-USSR R&D.

Gao, Q. (2015). Development of Laboratory and Field Drilling Tools to Measure Bit Operating Conditions and Drill String Motions. St. John's: Memorial University of Newfoundland.

Heng Li, S. B. (2010). Experimental Investigation of Bit Vibration on Rotary Drilling Penetration Rate. St John's: American Rock Mechanics Association.

Khademi, M. (2014). *Laboratory Study of the effect of Axial Compliance on Rock Peneteration of PDC Bits.* St. John's.

Khorshidian, H. M. (2012). The Role of Natural Vibrations in Penetration Mechanism of a Single PDC Cutter. *American Rock Mechanics Association.* Chicago.

Li, H. (2011). Experimental investigation of the rate of penetration of vibration assisted rotary drilling. *ARMA,* (pp. Unpublished manuscript, available at the Memorial University Library and the Drilling Technology Laboratory). Salt Lake City, UT.

McMater-Carr. (n.d.). *McMaster-Carr Supply Company*. Retrieved 03 16, 2019, from https://www.mcmaster.com/1290n37

Pessier, R., Walace, S., Oueslati, H., & Baker Hughes. (2012). Drilling Performance Is a Function of Power at the Bit and Drilling Efficiency. *SPE JPT,* 6.

R.Feenstra, J. L. (1964). Full-Scale Experiments on Jets in Impermeable Rock Drilling. *SPE, 16*(03), 329-336.

Rana, P. A. (2015). Experimental Evaluation of passive-Vibration Assisted Rotary Drilling. *American Rock Mechanics Association.* San Francisco.

Reyes, R., Kyzym, I., Rana, P., Molgaard, J., & Butt, S. (2015). *Cuttings Analysis for Rotary Drilling Penetration Mechanisms and Performance Evaluation.* San Francisco: American Rock Mechanics Association.

Shock Sub Tool Increases ROP 50%, Reduces Axial Vibrions While Drilling 22-in and 16-in Sections. (2015). Schlumberger.

Taylor, M. R., Murdock, A. D., Evans, S. M., & Hycalog. (1996). High Penetration Rates and Extended Bit Life through Revolutionay Hydraulic and Mechanical Design in PDC Drill Bit Developmet. *SPE Annual Technical Conference and Exhibition* (p. 14). Denver: SPE.

Wang, L., Butt, S., & Yang, J. (2013). DYNAMIC ANALYSIS OF BOTTOM HOLE ASSEMBLY WITH EXTERNAL VIBRATING. *Proceedings of the ASME 2013 International Mechanical Engineering Congress and Exposition.* San Diego.

Wilmot, G. M., Harjadi, Y., Langdon, S., Gagneaux, J., SPE, & Chevron Corp. (2010). Drilling Efficiency and Rate of Penetration - Definitions, Influencing Factors, Relationships and Value. *IADC/SPE Drilling Conference and Exhibition* (p. 13). New Orleans: IADC/SPE.

Xiao, Y., Abugharara, A., & Butt, S. (2019). *Experimental Measurement of pVARD Spring Load-Deflection and Prediction Calibration Using MITCalc.* St. John's.

Yusuf Babatunde, S. B. (2011). Investigation of the Effects of Vibration Frequency on Rotary Drilling Penetration Rate Using Diamond Drag Bit. *US Rock Mechanics / Geomechanics Symposium.* San Francisco: American Rock Mechanics Association.

Zhong, J., Yang, J., & Butt, S. (2016). DEM Simulation of Enhancing Driling Penetration USing Bivration and Experimental Validation. *Summer Simulation Multi-Conference.* Mondreal, Canada: Society for Modeling & Simulation International.

Appendix A: Calculations

A-1 Key Strength Calculation

To determine the shear through the keys that transmit the rotational force between the layers of the laboratory scale tool the total shear area of the tools is calculated and compared to the force generated from the torque on the tool at the radius of the shear planes of the keys. Once the shear stress is determined it can be compared to the yield stress of the material to calculate the safety factor of the design.

$t_{key} := 0.373\ in$ $OD_{shaft} := 2.5\ in$ $T_{Drill\_Max} := 80\ N \cdot m$

$l_{key} := 1.87\ in$ $n_{keys} := 4$

$\sigma_{yield} := 40000\ psi$ $\tau_{yield} := \frac{\sigma_{yield}}{\sqrt{3}} = 23094.011\ psi$

$A_{shear} := (l_{key} - t_{key}) \cdot t_{key} = 0.558\ in^2$ $F_{Key\_shear} := \frac{T_{Drill\_Max}}{\frac{OD_{shaft}}{2}} = 566.448\ lbf$

$\tau_{key\_shear} := \frac{F_{Key\_shear}}{A_{shear}} = 1014.447\ psi$

$SF_{key} := \frac{\tau_{yield}}{\tau_{key\_shear}} = 22.765$ $SF_{n\_keys} := \frac{\tau_{yield}}{\frac{\tau_{key\_shear}}{n_{keys}}} = 91.061$

A-2 O-Ring Gland Sizing

The laboratory scale tool has a set of piston O-Rings to seal the drilling fluid in the drill string. Below is a sample calculation for the compression of the 113 O-Ring in the tool. Parker's O-Ring handbook suggests an approximate 8% compression on a dynamic O-Ring. The below calculation determines both the concentric and eccentric compression of the O-Ring by the gland considering the tolerances on the mechanical parts.

$OD_{gland} := 0.588\ in$ $Tol_{gland} := -0.005\ in$ 113 O-Ring

$OD_{mandrel} := 0.748\ in$ $Tol_{mandrel} := -0.005\ in$ $ID_{oring} := 0.549$ $Tol_{oringID} := 0.007\ in$

$ID_{bore} := 0.75\ in$ $Tol_{bore} := 0.005\ in$ $CS_{oring} := 0.103\ in$ $Tol_{oringCS} := 0.003\ in$

$$GH := \frac{\left(\left(ID_{bore} + Tol_{bore}\right) - \left(OD_{gland} + Tol_{gland}\right)\right)}{2} = 0.086\ in$$ Concentric Gland Height

$$Comp_{con} := \left(\frac{\left(CS_{oring} - Tol_{oringCS}\right)}{GH} - 1\right) \cdot 100 = 16.279\ \%$$ Concentric Compression

$$GH_{ecc} := GH + \frac{\left(\left(ID_{bore} + Tol_{bore}\right) - \left(OD_{mandrel} + Tol_{mandrel}\right)\right)}{2} = 0.092\ in$$ Eccentric Gland Height

$$Comp_{ecc} := \left(\frac{\left(CS_{oring} - Tol_{oringCS}\right)}{GH_{ecc}} - 1\right) \cdot 100 = 8.696\ \%$$ Eccentric Compression

A-3 Belleville Washer Calculations for laboratory scale tool

Below are sample calculations for determining the spring constant for the Belleville washer springs stacked in series as well as a series stack of parallel sets, as used in the laboratory scale pVARD tool.

$P_{working} := 283\ lbf$ $\delta_{working} := 0.024\ in$ $k_{bellville} := \frac{P_{working}}{\delta_{working}} = 11791.667\ \frac{lbf}{in}$

Series Stack

$n_{series} := 5$ $k_{eq} := \left(\frac{1}{k_{bellville}} \cdot n_{series}\right)^{-1} = 2358.333\ \frac{lbf}{in}$

Parallel Series Stack

$n_{parallel} := 2$ $n_{series} := 5$

$k_{parallel} := k_{bellville} \cdot n_{parallel} = 23583.333\ \frac{lbf}{in}$ $k_{eq} := \left(\frac{1}{k_{parallel}} \cdot n_{series}\right)^{-1} = 4716.667\ \frac{lbf}{in}$

A-4 Loading capacity and safety factor for the keyed interface

This calculation is similar to that shown in A-1 but is applied to the rotational force of the field scale tool.

$t_{key} := 0.996\ in$ $OD_{shaft} := 2.98\ in$ $T_{Drill\_Max} := 8000\ ft \cdot lbf$

$l_{key} := 3.996\ in$ $n_{keys} := 12$

$\sigma_{yield} := 40000\ psi$ $\tau_{yield} := \frac{\sigma_{yield}}{\sqrt{3}} = 23094.011\ psi$

$A_{shear} := (l_{key} - t_{key}) \cdot t_{key} = 2.988\ in^2$ $F_{Key\_shear} := \frac{T_{Drill\_Max}}{\frac{OD_{shaft}}{2}} = 64429.53\ lbf$

$\tau_{key\_shear} := \frac{F_{Key\_shear}}{A_{shear}} = 21562.761\ psi$

$SF_{key} := \frac{\tau_{yield}}{\tau_{key\_shear}} = 1.071$ $SF_{n\_keys} := \frac{\tau_{yield}}{\frac{\tau_{key\_shear}}{n_{keys}}} = 12.852$

A-5 Torsion in top shaft and shell calculation

Building on previous calculation for the keys in the field scale tool the torsion taking ability of the two layers that make up the tool was calculated using the maximum torque that could be provided by the drilling rig used for the field trials.

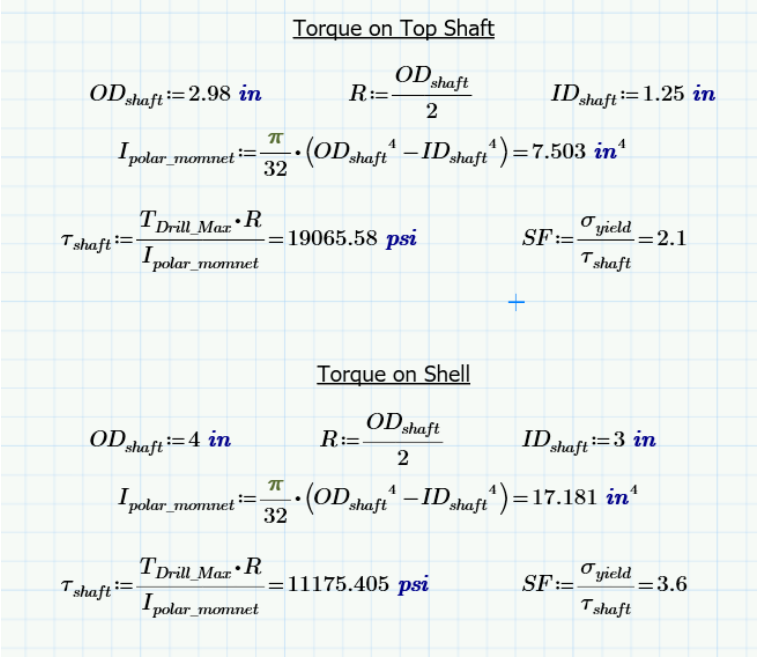

A-6 Buckling and compressive capacity of thin shaft section

One segment of the field scale tool that transmits the weight on bit seemed to be particularly thin, so it was checked for its ability to transmit axial compression as well as its resistance to buckling.

$OD_{shaft} := 2\ in$ $\quad R := \frac{OD_{shaft}}{2} = 1\ in$ $\quad F_{Max} := 30000\ lbf$

$ID_{shaft} := 1.25\ in$ $\quad r := \frac{ID_{shaft}}{2} = 0.625\ in$

$E := 207\ GPa$ $\quad I := \frac{\pi}{4} \cdot \left(R^4 - r^4\right) = 0.666\ in^4$

$K := 0.5$

$L := 714\ mm$

$F_{buckle} := \frac{\pi^2 \cdot E \cdot I}{(K \cdot L)^2} = 998312.838\ lbf$ $\quad SF := \frac{F_{buckle}}{F_{Max}} = 33.277$

$A_{CS} := \frac{\pi}{4} \cdot \left(OD_{shaft}^2 - ID_{shaft}^2\right) = 1.914\ in^2$

$F_{axial} := \sigma_{yield} \cdot A_{CS} = 76576.321\ lbf$ $\quad SF := \frac{F_{axial}}{F_{Max}} = 2.553$

A-7 Calculation of spring constant for field scale tool

Below are sample calculations for determining the spring constant for the Belleville washer springs stacked in series as well as a series stack of parallel sets, as used in the field scale pVARD tool.

$$P_{working} := 3120\ lbf \qquad \delta_{working} := .056\ in \qquad k_{belleville} := \frac{P_{working}}{\delta_{working}} = 55714.286\ \frac{lbf}{in}$$

Series Stack

$$n_{series} := 46 \qquad k_{eq} := \left(\frac{1}{k_{belleville}} \cdot n_{series}\right)^{-1} = 1211.18\ \frac{lbf}{in}$$

Parallel Series Stack

$$n_{parallel} := 3 \qquad n_{series} := 20$$

$$k_{parallel} := k_{belleville} \cdot n_{parallel} = 167142.857\ \frac{lbf}{in} \qquad k_{eq} := \left(\frac{1}{k_{parallel}} \cdot n_{series}\right)^{-1} = 8357.143\ \frac{lbf}{in}$$

A-8 Patent - Vibration assisted rotary drilling (VARD) tool

US publication Number: US 2017/0096862 A1

US010214972B2

(12) **United States Patent**
Butt et al.

(10) **Patent No.: US 10,214,972 B2**
(45) **Date of Patent: Feb. 26, 2019**

(54) **VIBRATION ASSISTED ROTARY DRILLING (VARD) TOOL**

(71) Applicants: **Stephen Butt**, St. John's (CA); **Brock Gillis**, Calgary (CA); **Pushpinder Singh Rana**, Pathankot Punjab (IN)

(72) Inventors: **Stephen Butt**, St. John's (CA); **Brock Gillis**, Calgary (CA); **Pushpinder Singh Rana**, Pathankot Punjab (IN)

(73) Assignee: **Memorial University of Newfoundland**, St. John's (CA)

(*) Notice: Subject to any disclaimer, the term of this patent is extended or adjusted under 35 U.S.C. 154(b) by 110 days.

(21) Appl. No.: **15/314,265**

(22) PCT Filed: **May 29, 2015**

(86) PCT No.: **PCT/CA2015/000345**

§ 371 (c)(1),
(2) Date: **Nov. 28, 2016**

(87) PCT Pub. No.: **WO2015/179953**

PCT Pub. Date: **Dec. 3, 2015**

(65) **Prior Publication Data**

US 2017/0096862 A1 Apr. 6, 2017

Related U.S. Application Data

(60) Provisional application No. 62/005,533, filed on May 30, 2014.

(51) **Int. Cl.**
E21B 17/07 (2006.01)
E21B 7/24 (2006.01)
(Continued)

(52) **U.S. Cl.**
CPC ***E21B 17/076*** (2013.01); ***E21B 3/00*** (2013.01); ***E21B 7/24*** (2013.01); ***E21B 12/00*** (2013.01)

(58) **Field of Classification Search**
CPC E21B 17/07; E21B 17/076; E21B 7/24
See application file for complete search history.

(56) **References Cited**

U.S. PATENT DOCUMENTS

4,276,948 A 7/1981 Hebel
4,502,552 A 3/1985 Martini
(Continued)

FOREIGN PATENT DOCUMENTS

GB 2486287 6/2012

OTHER PUBLICATIONS

Canadian Intellectual Property Office, International Search Report (Form PCT/ISA/210, 2 pgs.) and Written Opinion of the International Searching Authority (Form PCT/ISA/237, 4 pgs.), Jul. 14, 2015.

(Continued)

Primary Examiner — Giovanna C. Wright
(74) *Attorney, Agent, or Firm* — Wood Herron & Evans LLP

(57) **ABSTRACT**

Vibration assisted rotary drilling (VARD) tools that provide axial compliance and low amplitude axial displacements at the drill bit while transmitting the full rotary speed and torque of the drill string to increase drilling penetration rate. The VARD tools consist essentially of: i) an axially compliant section which transfers axial load across the tool; ii) a mechanism for opposing ends of the tool to displace axially relative to each other; iii) an energy absorbing section which dampens axial bit displacements; iv) a rotation transfer section which allows any rotation and torque applied to the drill string above the tool to be applied to the bit; and v) an optional axial force generating section.

7 Claims, 9 Drawing Sheets

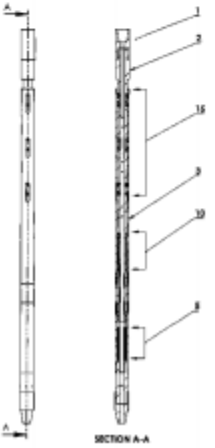

(51) **Int. Cl.**
E21B 3/00 (2006.01)
E21B 12/00 (2006.01)

(56) **References Cited**

U.S. PATENT DOCUMENTS

2014/0083772	A1	3/2014	Wiercigroch	
2016/0123090	A1*	5/2016	Schultz	E21B 7/24 166/381

OTHER PUBLICATIONS

Canadian Patent Office, Office Action issued in corresponding Canadian Patent Application No. 2,950,826, dated Sep. 13, 2017 (4 pages).
Canadian Patent Office, Office Action issued in corresponding Canadian Patent Application No. 2,950,826, dated Jul. 3, 2018 (5 pages).

* cited by examiner

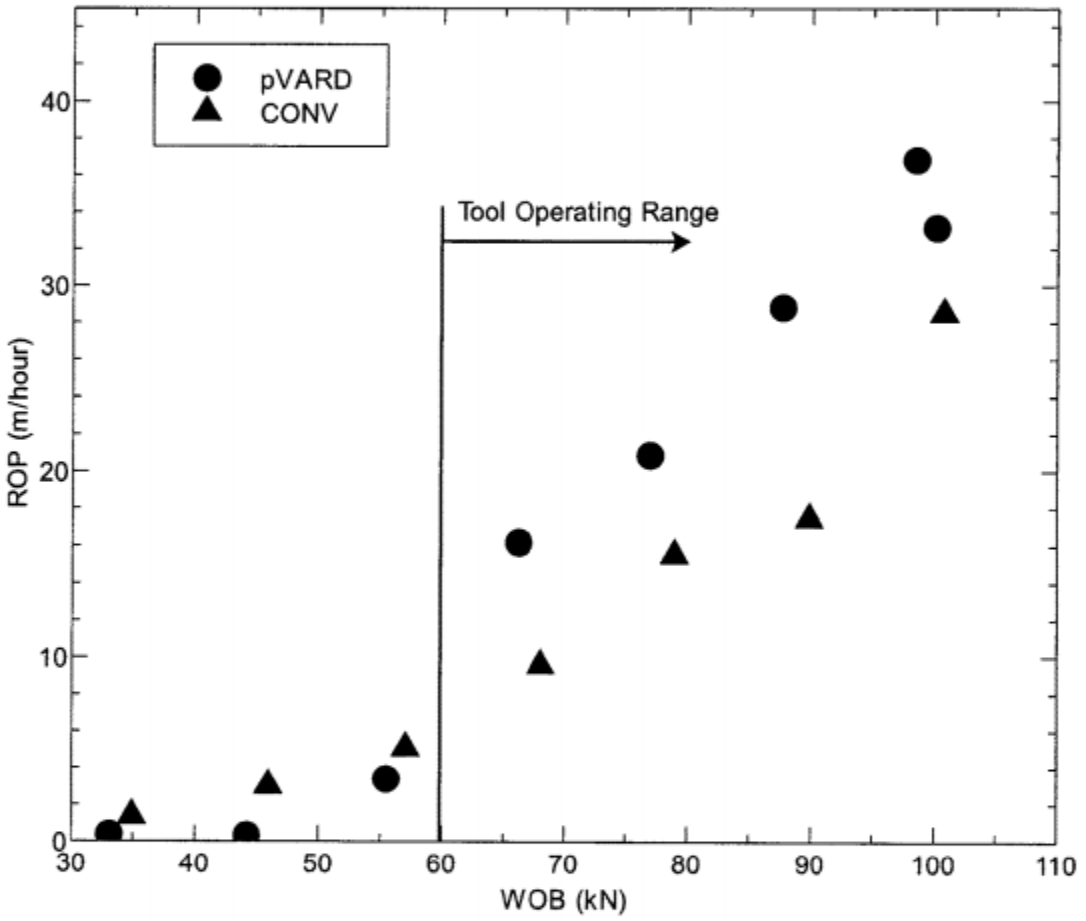
pVARD
CONV
Tool Operating Range
ROP (m/hour)
WOB (kN)
0
10
20
30
40
30
40
50
60
70
80
90
100
110

Figure 1

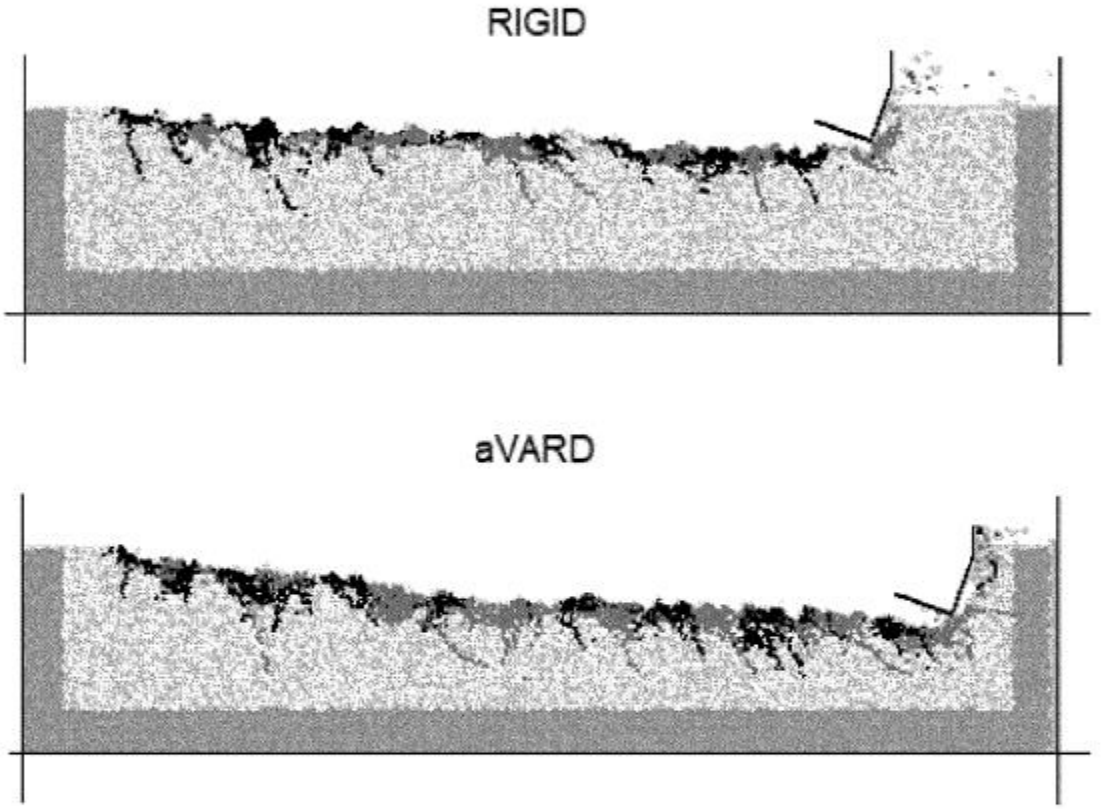

Figure 2

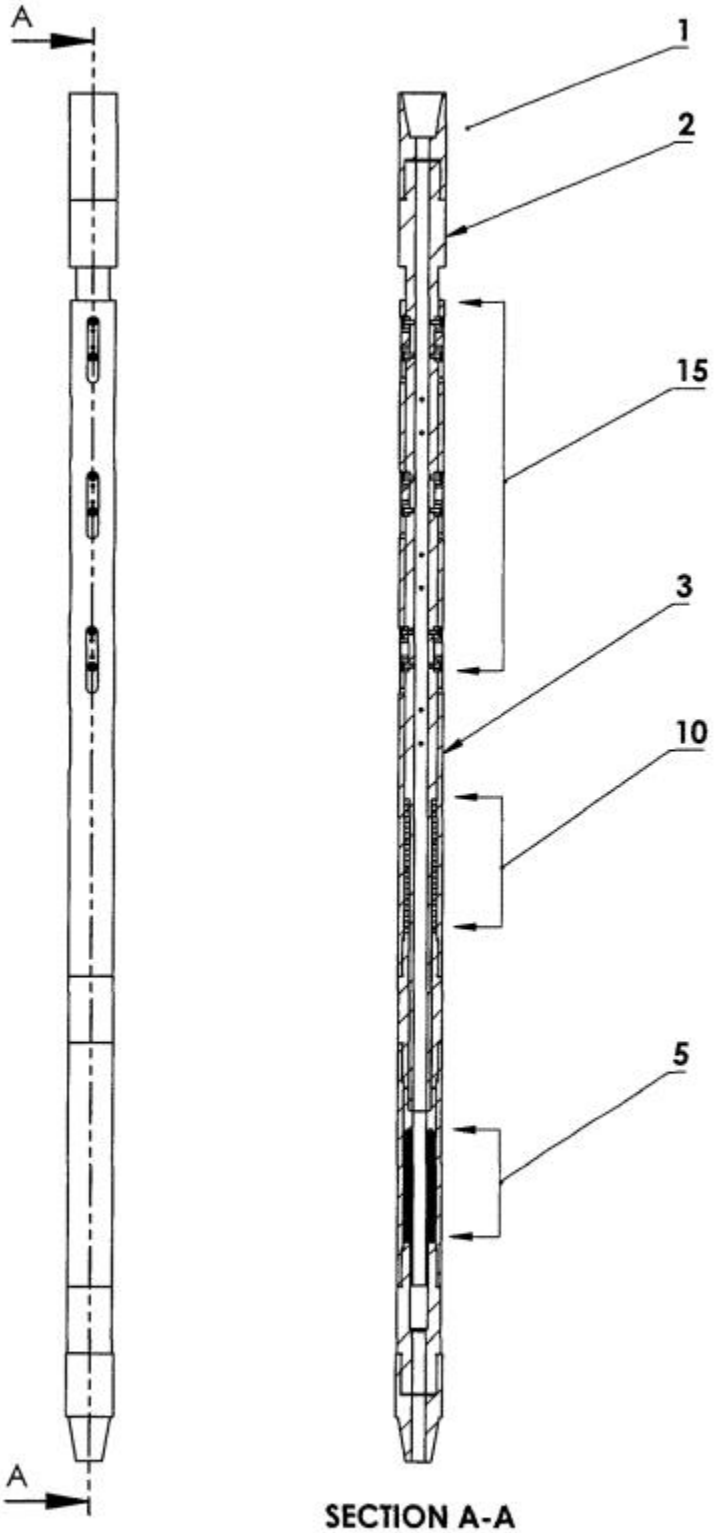

Figure 3

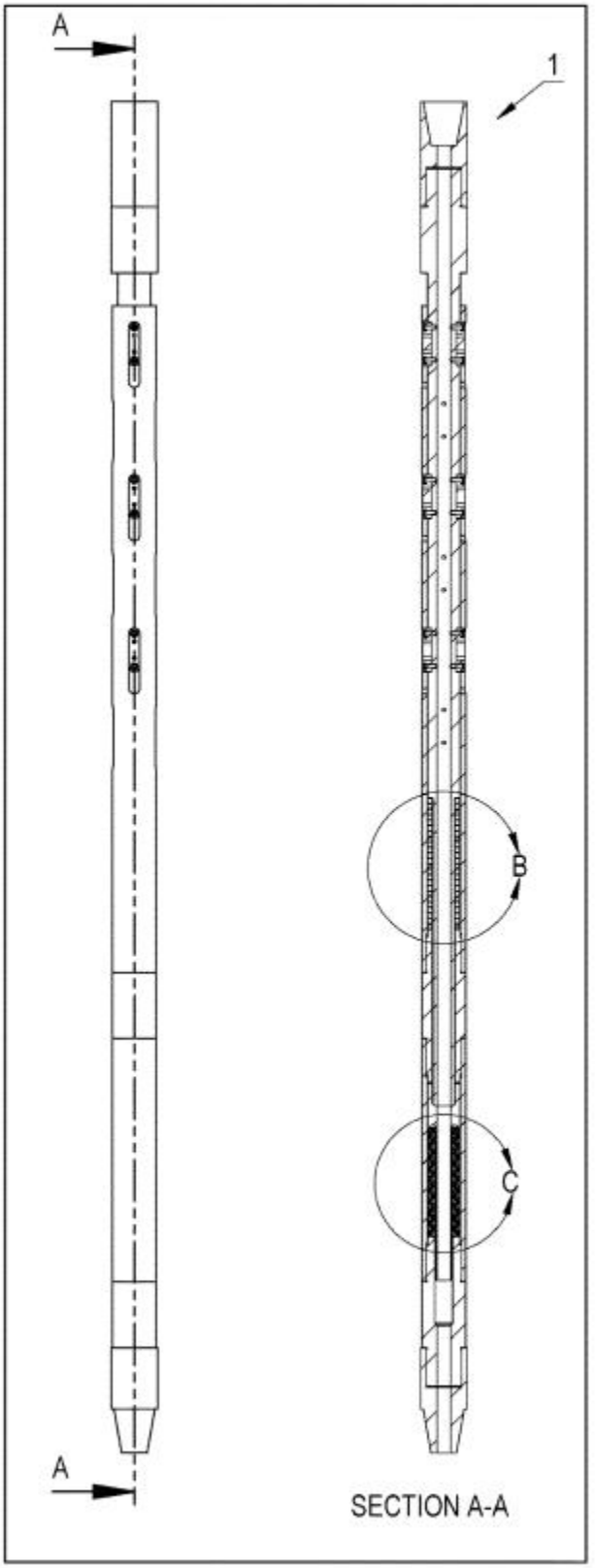

Figure 4A

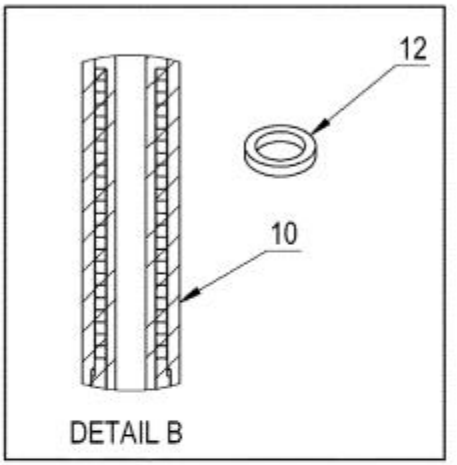

Figure 4B

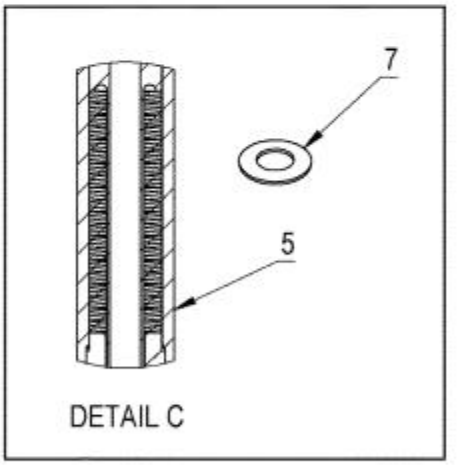

Figure 4C

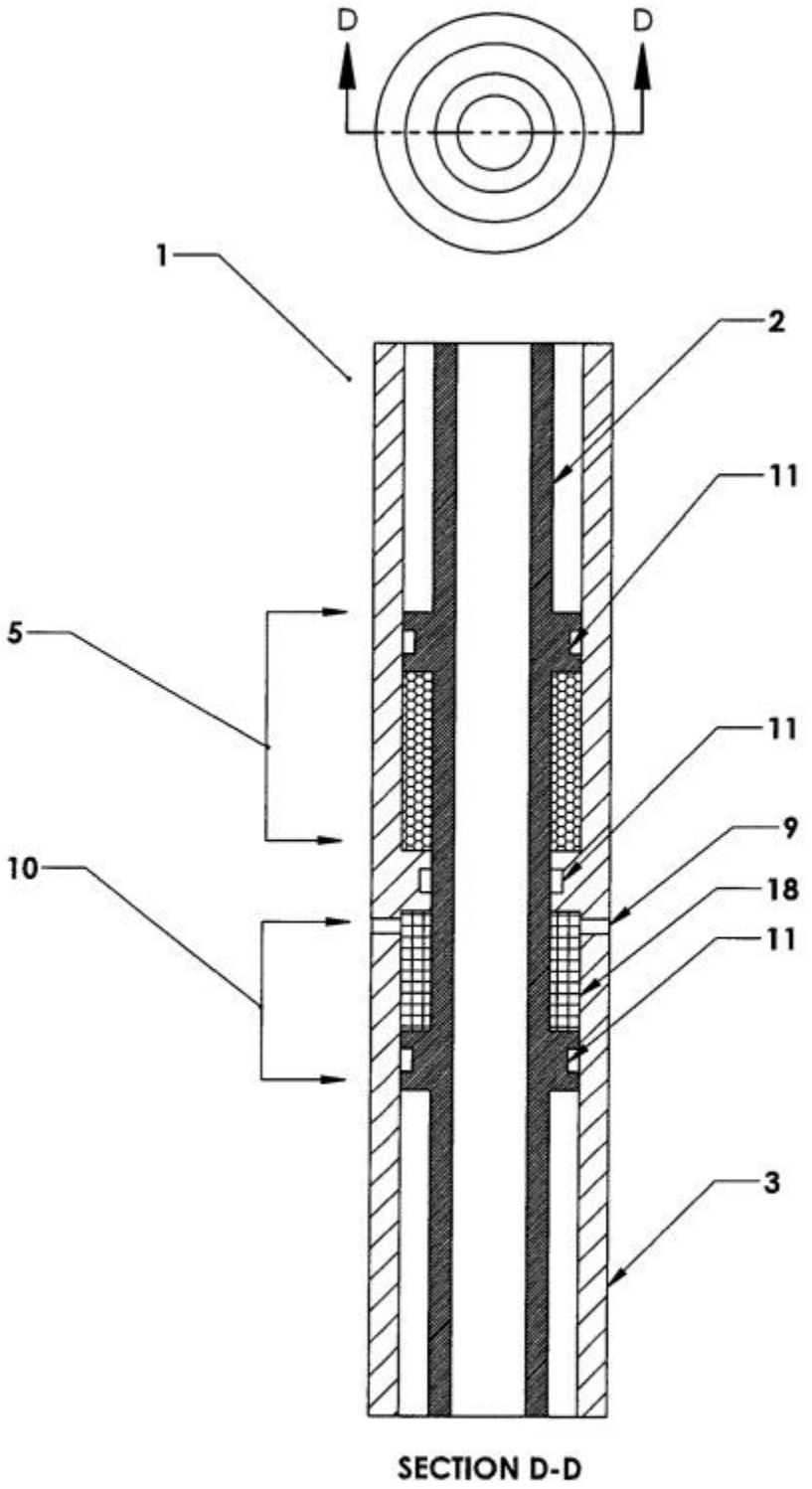

Figure 5

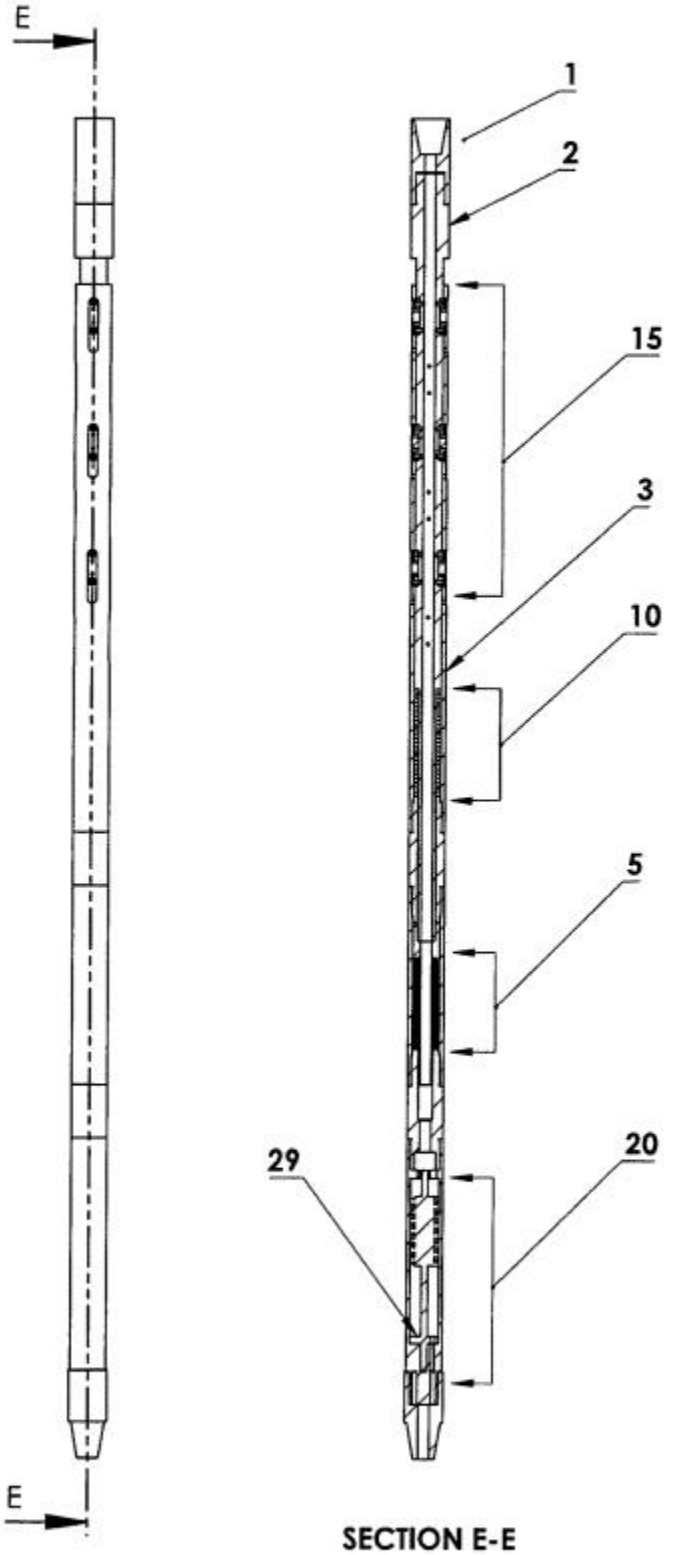

Figure 6

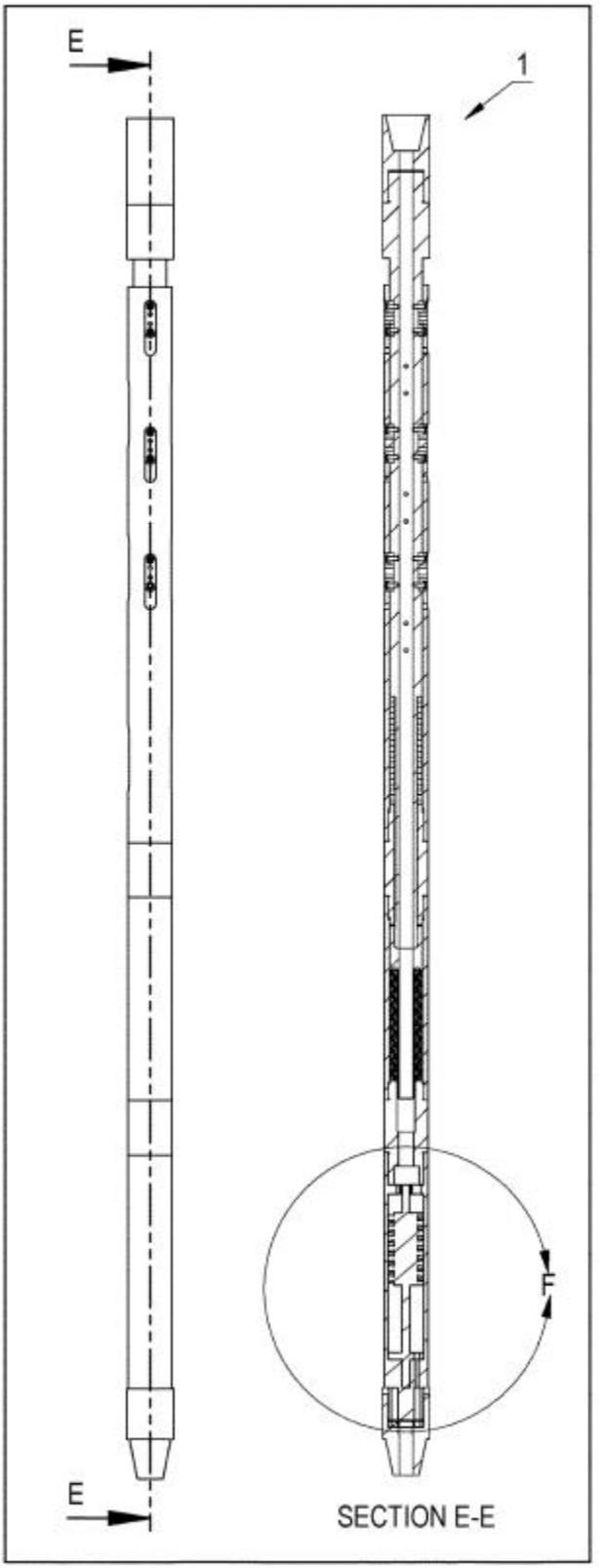

Figure 7A

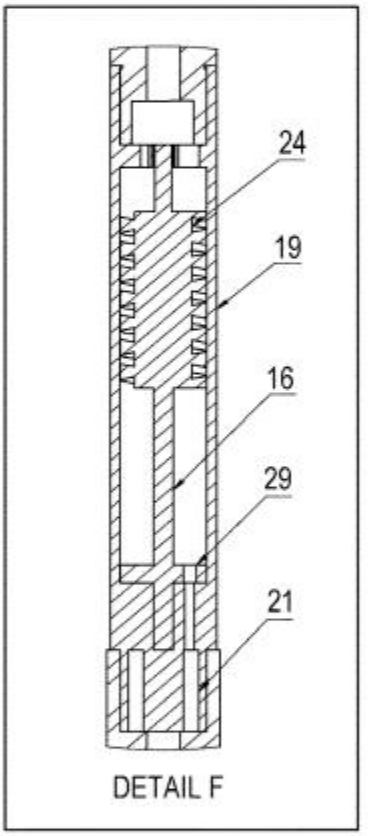

Figure 7B

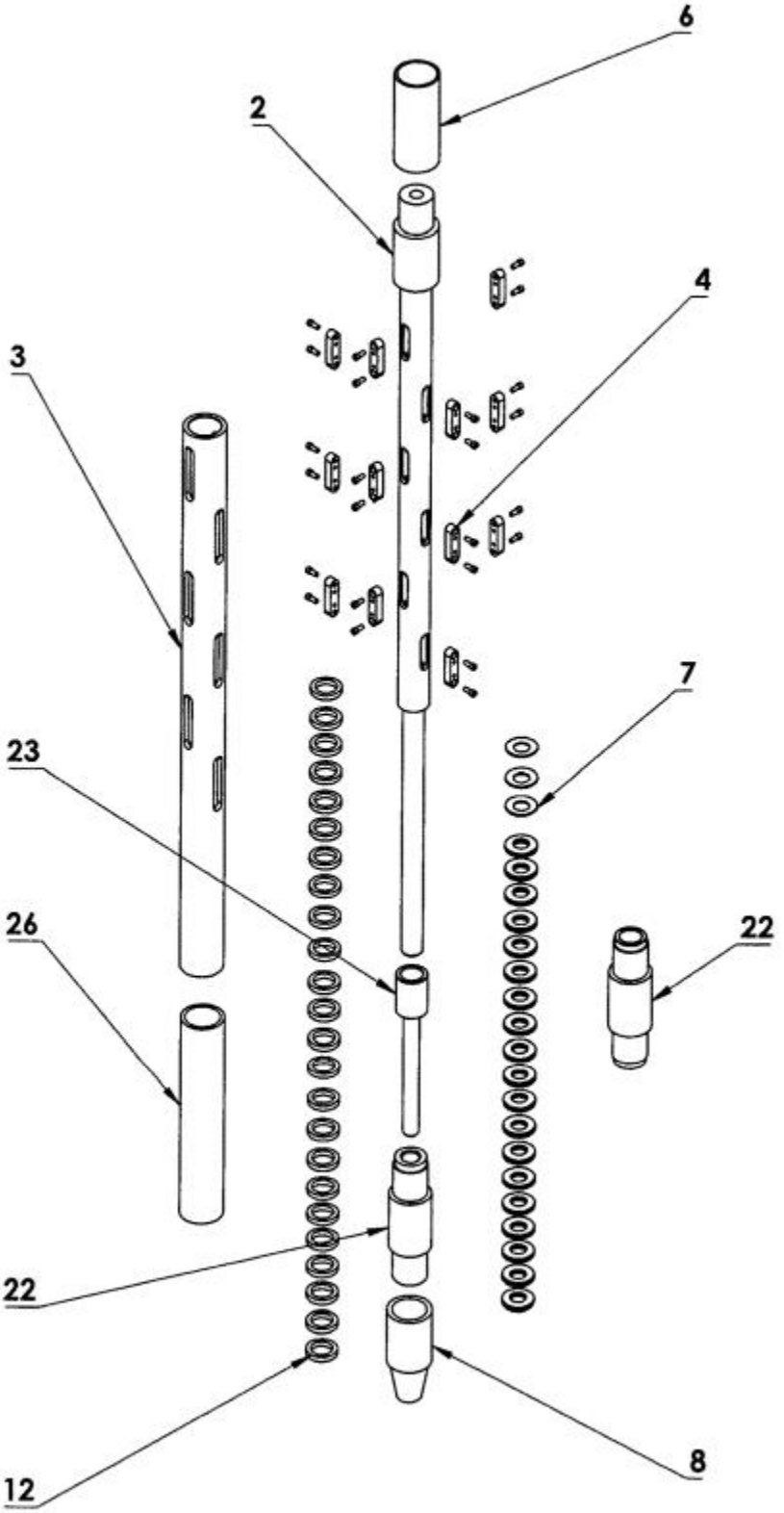

Figure 8

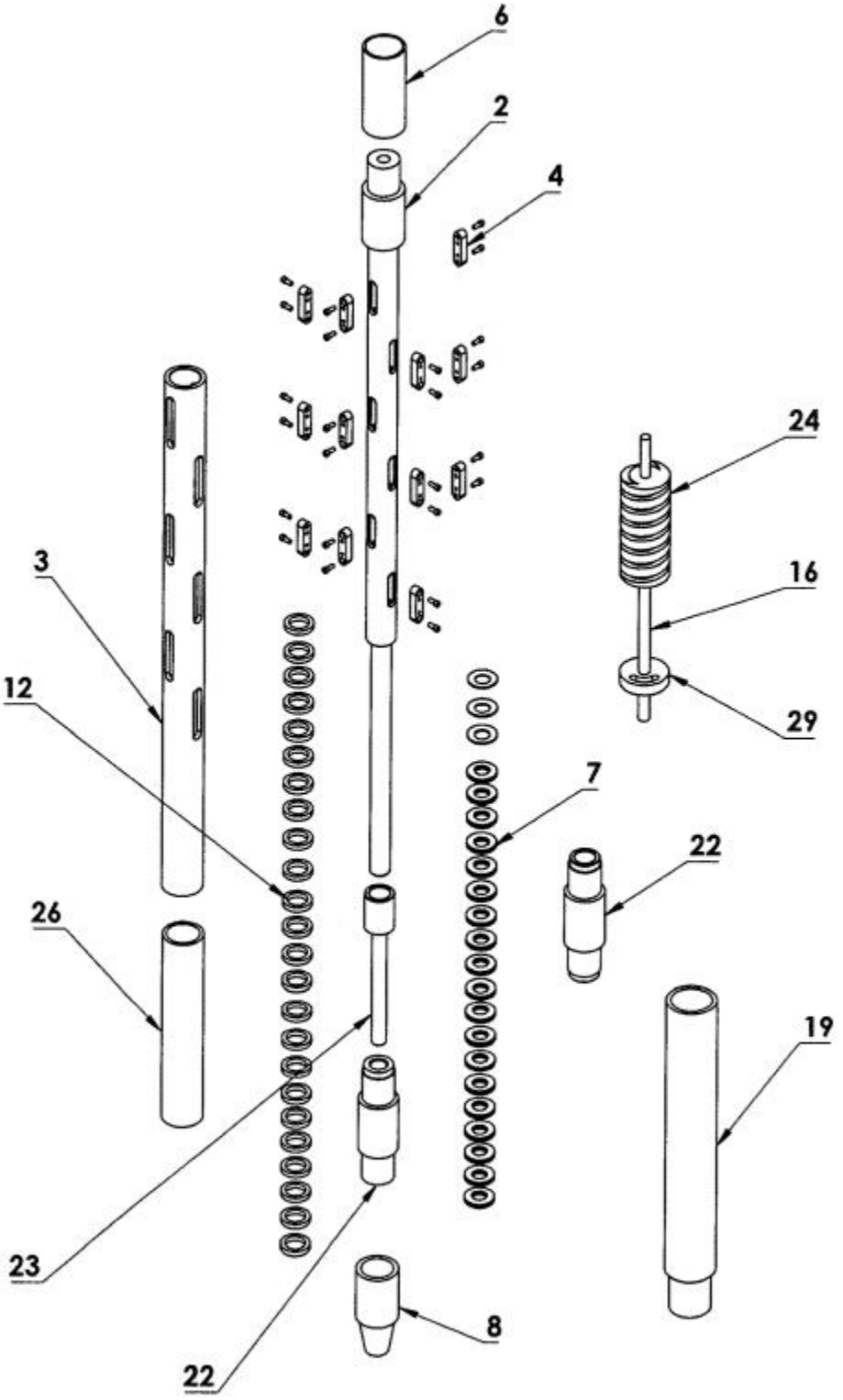

Figure 9

VIBRATION ASSISTED ROTARY DRILLING (VARD) TOOL

This application claims priority, under Section 371 and/or as a continuation under Section 120, to PCT Application No. PCT/CA2015/000345, filed on May 29, 2015, which claims priority to U.S. Provisional Application No. 62/005,533, filed on May 30, 2014.

FIELD OF THE INVENTION

The present invention relates to drilling tools. More particularly, the present invention relates to vibration assisted rotary drilling (VARD) tools.

BACKGROUND OF THE INVENTION

In conventional rotary drilling, a drill bit(s) is mounted on the end of a drill string, and a mixture of liquid and additives (drilling fluid or "mud") is pumped down the inside of the drill string and exits as fluid jets at the bit nozzles to cool and clean the bit, and flush the cuttings to the surface as the drill bit(s) grinds away at the rock formation. Drilling efficiency is generally governed by whether the rock cuttings are effectively removed by hydraulic forces of the drilling fluid jets.

Rotary drilling generally involves the application of axial force known as Weight-on-Bit ("WOB", the amount of downward force exerted on the drill bit), and rotary torque known as Torque-on-Bit ("TOB", the amount of rotational or turning force exerted on the drill bit), to push and rotate the drill bit to generate the cuttings. Unfortunately, it is well known that with increased depth, there is an increase in bottom hole pressure ("BHP") which holds the drill cuttings against the cutter face and the bottom of the hole, thereby impeding their efficient removal. This results in a reduction in the rate of penetration ("ROP") of the drill bit, and potentially increased well costs.

Currently, there are drilling tools which provide axial compliance in the drill string for the purpose of damping drill string vibration and shock in an attempt to overcome some vibration-related problems. These are typically called "shock subs" and are provided by several drilling technology companies. There are other drilling tools which provide axial force generation at the bit, but not in combination with axial compliance. There is no other drilling technology that specifically targets providing axial displacements at the drill bit through the use of axial compliance to allow the cuttings that are held down by the BHP to be displaced and removed more easily, and result in an increase in the drilling ROP. What is therefore needed is a novel, industrially viable, vibration assisted rotary drilling (VARD) tool that can increase ROP and drilling efficiency.

SUMMARY OF THE INVENTION

Disclosed are vibration assisted rotary drilling (VARD) tools which provide low amplitude axial displacements at the drill bit while applying WOB and transmitting the full rotary speed and torque of the drill string. These VARD Tools consist of: i) an axially compliant section which transfers axial load across the tool, ii) a mechanism for opposing ends of the tool to displace axially relative to each other, iii) an energy absorbing section which dampens axial bit displacements, iv) a rotation transfer section which allows the rotation and torque applied to a drill string above the tool to be applied to the drill bit, and v) an optional axial force generating section.

Under normal operating conditions, the VARD tool is installed in the Bottomhole Assembly ("BHA") directly behind the bit but can be installed further up in the BHA. Numerous manifestations of these 4 required and 1 optional components of the VARD tool can be achieved, using various types of materials and mechanical, hydraulic or pneumatic components. For example, most materials that comprise the body of the VARD tool would be alloys selected on the basis of strength and corrosion resistance, whereas energy absorbing/damping materials (used in item iii) would be selected from a variety of plastic, rubber or similar elastomers. Energy dampening can also be achieved by utilizing pressurized fluids in sealed chambers with interconnecting flow orifices. The axial force generating section (item v) can have various embodiments such as, but not limited to: a moving hydraulic valve assembly that periodically restricts the flow of drilling fluid acting on a pump open area ("POA") in the tool; a mechanically reciprocated or oscillated mass generating inertial reaction forces; an electro-magnetic mechanism which oscillates a magnetic mass or fluid; or a pulse cavitation mechanism which flows the drilling fluid through a venturi, generating cavitation bubbles which collapse and act on a POA in the tool. In the case of a VARD tool which does not include the optional axial force generating section (item v), the axially compliant section (item i) transforms just the natural axial forces generated by the cutting action of the drill bit cutters into axial displacement of the drill bit (this is hereinafter referred to as a passive VARD tool, with the ROP enhancement as shown in FIG. **1**). In the case where a VARD tool includes the optional axial force generating section (item v), the axially compliant section (item i) transforms both the axial forces produced by the axial force generating section and the natural axial forces produced by the cutting action of the drill bit cutters into axial displacement of the drill bit (this is hereinafter referred to as an active VARD tool, with the ROP enhancement as shown in FIG. **2**).

The tools of the present invention may be used to increase drilling ROP, increase drilling efficiency, or reduce the energy consumption per volume of penetrated rock.

BRIEF DESCRIPTION OF THE DRAWINGS

Various embodiments of the invention will now be described, by way of example, with reference to the accompanying drawings in which:

FIG. **1** is a chart showing ROP (m/hour) plotted against WOB (kN) comparing the results from field drilling experiments displaying the influence of a passive VARD tool wherein the data points for "pVARD" shows the higher ROP that was achieved at several WOB when a pVARD tool was included in the drilling BHA, and the data points for "CONV" showing the lower ROP that was achieved at similar WOB when no pVARD tool was employed.

FIG. **2** is a computerized display showing the results from a distinct element method ("DEM") model simulation of drag bit cutter penetration in rock showing the influence of an active VARD tool. For the image labeled "aVARD" the vertical force oscillations and the compliance of the active VARD tool were applied to the drag bit cutter, and for the image labelled as "RIGID" no active VARD tool was simulated.

FIG. **3** is a schematic representation of a passive VARD tool in accordance with one embodiment of the present invention.

FIG. **4** is a schematic representation of the energy absorbing and axially compliant sections, respectively, of the passive VARD tool shown in FIG. **3** in accordance with one embodiment of the present invention.

FIG. **5** is a schematic representation of the energy absorbing and axially compliant sections, respectively, of a passive VARD tool in accordance with a second embodiment of the present invention.

FIG. **6** is a schematic representation of an active VARD tool in accordance with a third embodiment of the present invention.

FIG. **7** is a schematic representation of the axial force generating section of an active VARD tool shown in FIG. **6** in accordance with a third embodiment of the present invention.

FIG. **8** is an exploded assembly drawing of a passive VARD tool shown in FIG. **3** in accordance with one embodiment of the present invention.

FIG. **9** is an exploded assembly drawing of an active VARD tool shown in FIG. **6** in accordance with a third embodiment of the present invention.

DETAILED DESCRIPTION OF THE INVENTION

The VARD tool of the present invention is capable of increasing drilling ROP, increasing drilling efficiency, and/or reducing the energy consumption per volume of penetrated rock. In particular, the VARD tool of the present invention is capable of overcoming the known problem of drilling ROP decreasing when the BHP increases with drilling depth. The present invention is therefore capable of increasing the ROP generally throughout the drilling operation, thus increasing drilling efficiency and reducing the time required to reach the drilling target, and thereby potentially reducing the overall costs associated with the drilling of a wellbore. This invention accordingly may have the added benefit of allowing drilling companies to drill more wells, including exploration wells, for similar drilling budgets.

In particular, through scientific laboratory investigation and field tests with our novel tool, we have discovered that low magnitude axial displacement of the drill bit allows for the cuttings that are held down by the BHP to be displaced and removed more easily, resulting in an overall increase in ROP. Drilling results were evaluated on the basis of ROP, mechanical specific energy ("MSE"), bit loads and bit displacements. The tool was tested both with and without compliance to evaluate the effects of the compliant element. FIG. **1** shows our results from field drilling experiments displaying the influence of a passive VARD tool (i.e. one that does not contain an axial force generating section, described below). The data points denoted as "pVARD" show the higher ROP that was achieved when a passive VARD tool was used in the drilling system and the WOB was within the operational range of the tool, as compared to the data points for "CONV" when no passive VARD tool was employed. FIG. **2** shows our results from a distinct element method ("DEM") model simulation of drag bit cutter penetration in rock, displaying the influence of an active VARD tool (i.e. one containing an axial force generating section, described below). In particular, the upper part of the figure labelled "RIGID" shows the cutter penetration without using an active VARD tool, while the lower part of the figure labeled "aVARD" shows the higher penetration achieved when an active VARD tool is used; otherwise, all other drilling parameters were the same.

The VARD tool **1** would normally be housed in an outer shell **3**, and consists of: i) an axially compliant section **5** which transfers axial load across the tool **1**, ii) a mechanism for opposing ends of the tool to displace axially relative to each other, iii) an energy absorbing section **10** which dampens axial bit displacements, and iv) a rotation transfer section **15** which allows the rotation and torque applied to a drill string above the tool **1** to be applied to the bit (these 4 items alone providing a passive VARD tool as shown, for example, in FIG. **3**), as well as v) an optional axial force generating section **20** (the addition of which provides an active VARD tool as shown, for example, in FIG. **6**). The axially compliant section **5** may contain stacks of Belleville washers **7** (as shown in FIG. **4**) or springs (or other similar material known to persons skilled in the art) or pressurized fluid that transfers the axial force from the top to the bottom of the tool **1** while allowing axial vibration to occur. The mechanism for opposing ends of the tool **1** to displace axially relative to each other may be achieved by use of an inner shaft **2** and an outer shell **3**, as shown in FIG. **3**. The energy absorbing section **10** contains dampening material that is capable of absorbing axial vibration energy, which may also be done through the use of hydraulic dampening. The rotation transfer section **15** allows the outer shell **3** of the tool **1** to move axially with respect to the inner shaft **2** of the tool **1**, while transferring rotary power through the use of keyways **4** (as shown in FIG. **8**) or a spline. The optional axial force generating section **20** is shown in FIG. **7** as comprising a valve assembly **29** mounted on the turbine shaft **16** that rotates with the turbine **24** and acts to vary the orifice of the valve assembly **29** to alternately reduce and increase the flow rate of drilling fluid flowing through the tool, resulting in pressure fluctuations that act on the POA **21** of the tool to generate axial force on a bit (although several other potential embodiments for axial force generating section **20** are described below).

Under normal operating conditions, the VARD tool is installed in the Bottomhole Assembly ("BHA") directly behind the drill bit but can be installed further up in the BHA. Numerous manifestations of these 4 required and 1 optional components of the VARD tool can be achieved, using various types of materials and mechanical, hydraulic or pneumatic components. For example, most materials that comprise the body of the VARD tool would be alloys selected on the basis of strength and corrosion resistance, whereas energy absorbing/damping materials (used in item iii, the energy absorbing section **10**) would be selected from a variety of plastic, rubber or similar elastomers. Energy dampening can also be achieved by utilizing pressurized fluids in sealed chambers with interconnecting flow orifices, as would be known to persons skilled in the art. The axial force generating section **20** (item v) can have various embodiments that would be known to persons skilled in the art, such as, but not limited to: a moving hydraulic valve assembly that periodically restricts the flow of drilling fluid acting on a POA in the tool; a mechanically reciprocated or oscillated mass generating inertial reaction forces; an electro-magnetic mechanism which oscillates a magnetic mass or fluid; or a pulse cavitation mechanism which flows the drilling fluid through a venturi, generating cavitation bubbles which collapse and act on a POA in the tool. In the case of a VARD tool **1** which does not include the optional axial force generating section **20** (item v), the axially compliant section **5** (item i) transforms just the natural axial forces generated by the cutting action of the drill bit cutters

into axial displacement of the drill bit (this is a passive VARD tool, with the ROP enhancement as shown in FIG. **1**). In the case where a VARD tool **1** includes the optional axial force generating section **20** (item v), the axially compliant section **5** (item i) transforms both the axial forces produced by the axial force generating section **20** and the natural axial forces produced by the cutting action of the drill bit cutters into axial displacement of the drill bit (this is an active VARD tool, with the ROP enhancement as shown in FIG. **2**).

FIG. **3**, as mentioned, displays a schematic representation of a passive VARD tool in accordance with one embodiment of the present invention. In this embodiment, the VARD tool **1** comprises a hollow inner shaft **2** and outer shell **3** that provides relative movement (axial displacement) between opposing ends of the tool (i.e. item 2, the mechanism for opposing ends of the tool to displace axially relative to each other). More specifically, inner shaft **2** transfers torque and load from the drill string to the outer shell **3**, while outer shell **3** transfers torque and axial load back to the drill string. Also in this embodiment, the axially compliant section **5** comprises stacks of Belleville washers **7** or coil springs to provide axial compliance, an elastomer/dampening material is used in the energy absorbing section **10** to provide energy absorption dampening, and a keyways **4**/spline section is used within the rotation transfer section **15** to provide rotation transfer. FIG. **4** provides a schematic representation of the energy absorbing section **10** and axially compliant section **5**, respectively, of the passive VARD tool as shown in FIG. **3** in accordance with one embodiment of the present invention. The axially compliant section **5** is shown comprising stacks of Belleville washers **7** or coil springs to transfer axial load (for axial compliance), while the energy absorbing section **10** is shown employing stacked rings of energy absorbing material **12** for dampening vibration (which could also be done using hydraulic dampening). FIG. **5** provides a schematic representation of the energy absorbing section **10** and axially compliant section **5** of a passive VARD tool as shown in FIG. **3** in accordance with a second embodiment of the present invention. In this embodiment, the passive VARD tool uses hydraulic mechanisms for both axial compliance and energy dampening. Here, the axially compliant section **5** contains pressurized fluid that transfers the axial force from the top to the bottom of the tool **1** while allowing axial vibration to occur; the energy absorbing section **10** is shown as a sealed piston chamber **18** with orifices **9** to the drilling fluid contained within the outer shell **3**. Fluid flow through these orifices **9** act as a dampener to absorb axial vibration energy. Shaft seals **11** prevent the pressurized fluid from travelling between the piston chamber **18** and the outer shell **3** except through the orifices **9** which restricts the fluid flow rate and the axial piston movement thus dampening the axial displacement. Once again, inner shaft **2** transfers torque and load from the drill string to the outer shell **3**, while outer shell **3** transfers torque and axial load back to the drill string.

FIG. **6** displays a schematic representation of an active VARD tool in accordance with a third embodiment of the present invention. In this embodiment, the VARD tool **1** comprises a hollow inner shaft **2** and outer shell **3** that provides relative movement (axial displacement) between opposing ends of the tool (i.e. item 2, the mechanism for opposing ends of the tool to displace axially relative to each other). More specifically, inner shaft **2** transfers torque and load from the drill string to the outer shell **3**, while outer shell **3** transfers torque and axial load back to the drill string. Also in this embodiment, the axially compliant section **5** comprises stacks of Belleville washers **7** or coil springs to provide axial compliance, an elastomer/dampening material is used in the energy absorbing section **10** to provide energy absorption dampening, a keyways/spline section is used within the rotation transfer section **15** to provide rotation transfer, and an axial force generating section **20** is used to apply axial force on a drill bit. FIG. **4** provides a schematic representation of the energy absorbing section **10** and axially compliant section **5**, respectively, as they could also be in the active VARD tool as shown in FIG. **6** in accordance with the third embodiment of the present invention. The axially compliant section **5** is shown comprising stacks of Belleville washers **7** or coil springs to transfer axial load (for axial compliance), while the energy absorbing section **10** is shown employing stacked rings of energy absorbing material **12** for dampening vibration (which could also be done using hydraulic dampening). FIG. **7** provides a schematic representation of the axial force generating section **20** as comprising a valve assembly **29** mounted on turbine shaft **16** that acts to vary the opening of the orifice of the valve assembly **29** when it is rotated by turbine **24** to alternately reduce and increase the flow rate of drilling fluid flowing through the tool, resulting in pressure fluctuations that act on the tool POA **21** to generate axial force on a bit (although several other potential embodiments for axial force generating section **20** are available as described previously). The axial compliant section **5** permits the axial forces acting on the bit to result in axial bit displacements, and the frequency and amplitude of these axial displacements can be adjusted by changing the configuration of the valve assembly **29**, the axially compliant section **5** and/or the energy absorbing section **10**, as would be known by a person skilled in the art.

FIG. **8** and FIG. **9** present exploded assembly drawings of the passive VARD tool shown in FIG. **3** and the active VARD tool shown in FIG. **6**, respectively, to provide persons skilled in the art with easy understanding of the mechanisms and assembly of these tools. FIG. **8** for the passive VARD tool shows API box connection **6** and the API pin connection **8** to mount the tool in the BHA, the outer shell **3** and the hollow inner shaft **2** with keyways **4** to allow relative displacement between both ends of the tool and to transfer rotation, the Belleville washers **7** which are stacked on the spring stack mandrill **23** and the spring stack shell **26** which together comprise the axially compliant section **5**, the rings of energy absorbing material **12** that are stacked on the lower portion of the inner shaft **2** to provide axial dampening, and the threaded couplings **22** which connect the spring stack shell **26** to the outer shell **3** and the API pin connection **8**. FIG. **9** for the active VARD tool shows all the elements shown in FIG. **8** plus the components of the axial force generating section **20**, which is comprised of the axial force generator shell **19**, the turbine **24**, the turbine shaft **16** and the rotating valve assembly **29**.

We claim:

1. A vibration assisted rotary drilling (VARD) tool comprising:

i) an axially compliant section which transfers axial load across the tool;

ii) a mechanism for opposing ends of the tool to displace axially relative to each other;

iii) an energy absorbing section which is axially displaced from the axially compliant section and dampens axial bit displacements, and

iv) a rotation transfer section which allows any rotation and torque applied to a drill string above the tool to be applied to a drill bit,

wherein said VARD tool is capable of providing low amplitude axial displacements at the drill bit while

applying weight-on-bit and the drill string operates at full rotary speed and torque.

2. A vibration assisted rotary drilling (VARD) tool as claimed in claim **1** wherein the tool further comprises an axial force generating section.

3. The VARD tool as claimed in claim **2** wherein the axially compliant section transforms axial forces produced by the axial force generating section and natural axial forces produced by a cutting action of cutters of the drill bit into axial displacements of the drill bit.

4. The VARD tool as claimed in claim **2** wherein the axial force generating section comprises a moving hydraulic valve assembly that periodically restricts flow of drilling fluid acting on a pump open area in the tool.

5. The VARD tool as claimed in claim **1** wherein the VARD tool is installed in a bottomhole assembly (BHA) directly behind the drill bit.

6. The VARD tool as claimed in claim **1** wherein the VARD tool is installed in a bottomhole assembly (BHA) remote from the drill bit.

7. The VARD tool as claimed in claim **1** wherein the axially compliant section transforms natural axial forces produced by a cutting action of cutters of the drill bit into axial displacements of the drill bit.

* * * * *